HHS Public Access

Author manuscript

Cell Rep. Author manuscript; available in PMC 2022 January 14.

Published in final edited form as:

Cell Rep. 2021 December 28; 37(13): 110164. doi:10.1016/j.celrep.2021.110164.

Mobilization of vitamin B_{12} transporters alters competitive dynamics in a human gut microbe

Katie A. Frye[1], **Varadh Piamthai**[2], **Ansel Hsiao**[2], **Patrick H. Degnan**[2,3,*]

[1]Department of Microbiology, University of Illinois at Urbana-Champaign, Urbana, IL 61801, USA

[2]Department of Microbiology and Plant Pathology, University of California, Riverside, Riverside, CA 92521, USA

[3]Lead contact

SUMMARY

The functional and genomic diversity of the human gut microbiome is shaped by horizontal transfer of mobile genetic elements (MGEs). Characterized MGEs can encode genes beneficial for their host's self-defense (e.g., antibiotic resistance) or ability to compete for essential or limited resources (e.g., vitamins). Vitamin B_{12} and related compounds (corrinoids) are critical nutrients that enable colonization by members of the common gut microbe phylum, the Bacteroidetes. Herein, we identify a distinct class of MGEs in the Bacteroidetes responsible for the mobilization and exchange of the genes required for transport of corrinoids, a group of cyclic tetrapyrrole cofactors including vitamin B_{12} (*btuGBFCD*). This class includes two distinct groups of conjugative transposons (CTns) and one group of phage. Conjugative transfer and vitamin B_{12} transport activity of two of the CTns were confirmed *in vitro* and *in vivo,* demonstrating the important role MGEs play in distribution of corrinoid transporters in the Bacteroidetes.

Graphical abstract

*Correspondence: patrick.degnan@ucr.edu.

AUTHOR CONTRIBUTIONS

K.A.F. and P.H.D. conceptualized the study; K.A.F. and P.H.D. developed the methodology; P.H.D. developed the software; K.A.F. and P.H.D. validated the study; K.A.F. and P.H.D. performed formal analysis; K.A.F., V.P., and P.H.D. performed study investigation; P.H.D. and A.H. obtained resources; P.H.D. performed data curation; K.A.F. wrote the original draft; K.A.F, A.H., and P.H.D. reviewed and edited the manuscript; K.A.F. and P.H.D. visualized the study; P.H.D supervised the study; A.H. and P.H.D. acquired the funding.

SUPPLEMENTAL INFORMATION

Supplemental information can be found online at https://doi.org/10.1016/j.celrep.2021.110164.

DECLARATION OF INTERESTS

The authors declare no competing interests.

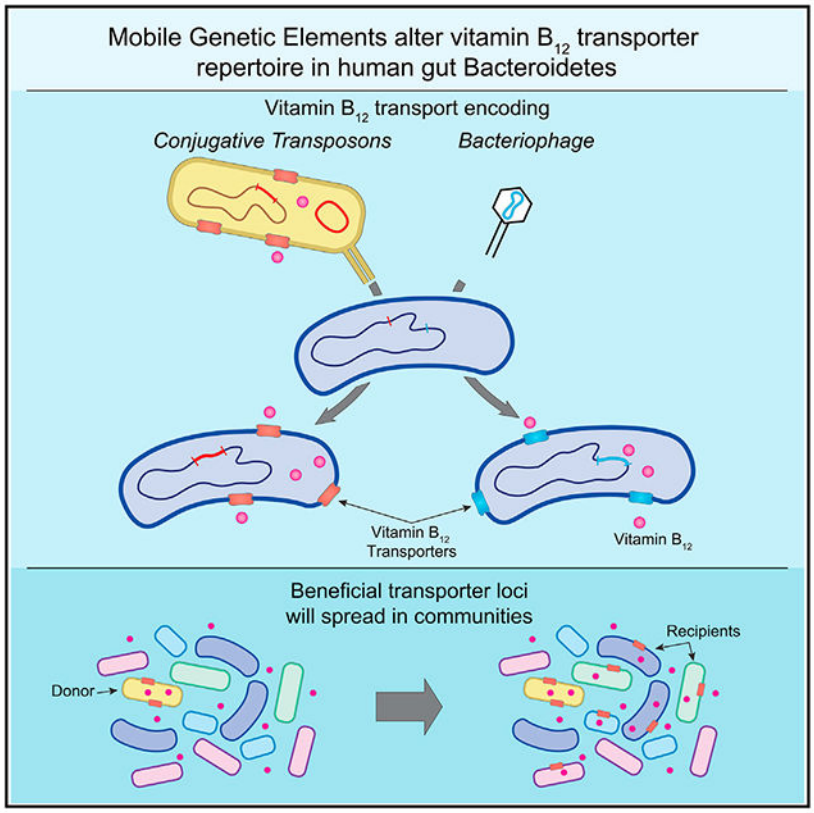

In brief

Mobile DNA can improve the competitive abilities of microbes. Frye et al. identify three distinct families of mobile DNA that encode vitamin B_{12} transporters in human gut Bacteroidetes. *In vitro* and *in vivo* transfer experiments demonstrate the importance of HGT in shaping competition for essential small molecules like B_{12}.

INTRODUCTION

The Bacteroidetes are prominent members of the human gut microbiota that comprise as much as 80% of the microbiome in some individuals (The Human Microbiome Project, 2012). Importantly, the Bacteroidetes play roles in different aspects of human health, including metabolism, obesity, inflammatory bowel disease, development of the immune system, and protection against colonization by invading pathogens (Buffie and Pamer, 2013; Hong and Rhee, 2014; Jacobson et al., 2018; John and Mullin, 2016; Kamada et al., 2012; Rowland et al., 2018; Sequeira et al., 2020; Sommer and Bäckhed, 2013; Visconti et al., 2019; Wikoff et al., 2009). To colonize the human gut, microbes must compete for essential resources, such as vitamins. This includes vitamin B_{12} and related compounds termed corrinoids (Degnan et al., 2014a; Goodman et al., 2009). As a cofactor, corrinoids are critical in many enzymatic reactions, including those involved in amino acid synthesis, nucleotide synthesis, and metabolism (Chimento et al., 2003; Roth et al., 1996). As such,

corrinoid transporters are key for colonization by a majority of gut microbes (Degnan et al., 2014b; Goodman et al., 2009).

Microbially produced corrinoids can be abundant in the large intestines and are structurally diverse with as many as eight distinct corrinoids found in a single patient sample (Allen and Stabler, 2008). This structural diversity of corrinoids is matched by corrinoid transporter sequence diversity (Degnan et al., 2014b). Microbes with distinct corrinoid cofactor preferences can possess specific transport capabilities, specific synthesis or remodeling capabilities, or a combination of these to accommodate their needs (Yi et al., 2012). Computational analyses revealed that of the 80% of gut microbes that encode corrinoid-dependent genes or riboswitches, only 20% encode complete, *de novo*, biosynthesis pathways without any ability to transport corrinoids (Degnan et al., 2014b). Therefore, most gut microbes must rely on transport to obtain and/or remodel these essential cofactors from dietary or microbial sources.

Corrinoid transport loci in the Bacteroidetes have components homologous to those in *Escherichia coli*, including an outer membrane transporter (BtuB), periplasmic binding protein (BtuF), and inner membrane ATP-dependent transporters (BtuC/D) (Di Girolamo and Bradbeer, 1971; Kenley et al., 1978). Unlike *E. coli,* Bacteroidetes transport operons also include a novel family of surface-exposed lipoproteins (BtuG), critical for binding extracellular corrinoids and essential for efficient transport via BtuB (Wexler et al., 2018). Furthermore, many of the Bacteroidetes encode multiple corrinoid transport loci, with the type strain *Bacteroides thetaiotaomicron* VPI-5482 encoding three homologous loci, Locus 1, Locus 2, and Locus 3 (Degnan et al., 2014b). Locus 1 encodes only the outer membrane transporter and lipoprotein, *btuGB,* while Locus 2 and Locus 3 encode complete *btu* transport loci (*btuGBFCD*). These homologous loci are not redundant and, in fact, display distinct corrinoid preferences that confer competitive advantages depending upon the corrinoid present (Degnan et al., 2014b). Previous work comparing the corrinoid preference specifying outer membrane transporter (BtuB) phylogeny with the species phylogeny revealed that among the Proteobacteria, the BtuB and species phylogeny are similar, whereas the Bacteroidetes BtuB and species phylogenies are incongruent (Degnan et al., 2014b). This suggested that there has been duplication, divergence, and horizontal gene transfer (HGT) of these alleles among the Bacteroidetes.

The possibility of spread of these corrinoid transporters via HGT is likely, as there is widespread evidence for rampant HGT within the gut (Coyne et al., 2014; Hehemann et al., 2010; Meehan and Beiko, 2012; Shkoporov et al., 2013; Shoemaker et al., 2001). In gut Bacteroidetes, conjugative transposons (CTns) and phage are common and are major mechanisms for HGT. This has resulted in substantial genomic diversity at both the species and strain level (Shoemaker et al., 2001). When these mobile genetic elements (MGEs) are transferred, part of their success (e.g., persistence) in a new host depends upon their contribution to their host's fitness. For instance, a single MGE, CTnDOT, carries antibiotic resistance genes for erythromycin (*ermF*), tetracycline (*tetQ, tetX*), and streptomycin (*aadS*). Other Bacteroidetes CTns encode gene products that have alternate means of increasing the fitness of their host by altering cell attachment or engaging in interbacterial antagonism

(Coyne et al., 2014), and at least one Bacteroidetes phage can alter bile acid metabolism (Campbell et al., 2020).

In this study, we have identified a distinct class of MGEs including putative CTns and a phage within gut Bacteroidetes that encode putative corrinoid transport genes. Here, we have experimentally verified both the ability for two of the CTns to transfer to naïve hosts and the functionality of the MGE-encoded corrinoid transport locus to transport vitamin B_{12}. Furthermore, these CTns exhibit different fitness advantages when competing against the previously characterized *B. thetaiotaomicron* chromosomally encoded *btu* loci depending on which loci they are competing against. Finally, we determined that the CTns are capable of transferring within the murine intestine, suggesting these elements can be shared in the human gut and contribute to the diversity of corrinoid acquisition loci found in gut Bacteroidetes. Together, these data expose a distinct class of MGEs within the Bacteroidetes that encode and disseminate transport loci for an essential resource required for colonization by these prominent members of the human gut microbiome.

RESULTS

Distinct corrinoid transporters are encoded on three genetically divergent MGE families

Our previous work on chromosomally encoded corrinoid transport loci within *B. thetaiotaomicron* revealed a discordance between the Bacteroidetes species and BtuB phylogenies, raising the possibility of horizontal gene transfer (HGT) of *btuB* alleles among the Bacteroidetes (Degnan et al., 2014b). To determine the role of MGEs in *btuB* allele distribution, we examined 133 gut Bacteroidetes genomes and identified 19 putative MGEs encoding putative corrinoid transport loci (Tables 1, S1, and S2). Phylogenetic reconstruction of this expanded set of *btuB* alleles determined that all MGE-encoded BtuBs group within the previously delineated BtuB “Family N” (Figures 1A and S1) (Degnan et al., 2014b). Furthermore, the majority of MGE-encoded BtuBs are clustered on the phylogeny and are more similar to the *B. thetaiotaomicron* VPI-5482 chromosomally encoded BtuB2 rather than BtuB3 (Figures 1A and S1). Despite BtuB2 and BtuB3 both belonging to Family N, they have been previously demonstrated to have distinct corrinoid preferences (Degnan et al., 2014b).

In order to understand the relatedness of these corrinoid transport-encoding MGEs, the nucleotide similarity over the entirety of each of the elements was used to calculate pairwise percent length aligned (PLA), and these elements were clustered with the Markov Cluster Algorithm (Figure 1B) (Enright, 2002; van Dongen, 2000). This led to the generation of three distinct “families” of predicted corrinoid transport-encoding MGEs (Family 1–3, Figure 1B). We note that the well-characterized Bacteroidetes CTn, CTnDOT, was included in these relatedness analyses and found to have similarity to one of the corrinoid transport-encoding MGEs; however, given its lack of a corrinoid transport locus, it was not included in Family 2 (Figures 1B and S4). We also note that this limited similarity of Family 2 mating pair formation and DNA transfer replication genes also extends to CTnBST, CTnHyb, and other members of the CTnDOT/ERL family of antibiotic-resistant conjugative transposons (Husain et al., 2014; Wesslund et al., 2007).

In general, the predicted corrinoid transport-encoding MGEs grouped into families that mirror the BtuB phylogeny (Figures 1 and S1). All of the MGE-encoded BtuB alleles in Family 1 (except for *Bacteroides plebeius*) and Family 3 group separately from the chromosomally encoded BtuB2 and BtuB3 in *B. thetaiotaomicron* VPI-5482. The *B. plebeius* and Family 2 MGEs, however, encode BtuB alleles that are nearly identical to BtuB2 (*B. plebeius* BtuB: 95% identity, *B. stercoris* and *B. finegoldii* BtuB: 100% identity; Figures 1A and S1). In addition, examination of the predicted integrases for MGE families 1 and 3 reveals a high degree of conservation within each family. This conservation, however, is not detected in the Family 1 MGE from *B. plebeius* and the Family 2 MGEs. The *B. plebeius* MGE encodes an integrase that is greater than 80% similar to the one encoded by the Family 2 *B. finegoldii* MGE, sharing far less (67%–71%) homology to the integrases encoded by the other members of their respective MGE families (Figure 1B).

Annotation and analysis of the protein domains (PFAMs) and families (TIGRFAMs) present within the predicted MGEs allowed us to determine that Family 1 and 2 elements are likely CTns, while the Family 3 elements are likely integrated phage (Table S3). Alignments of the complete set of Family 1 MGEs exhibits extensive homology over the entire length of the MGEs; however, broad diversity within the Family 1 MGEs indicates they are related but unlikely to represent a single, recently transferred element (Figure S2). In contrast, three of the five predicted phages within Family 3 are nearly identical over their entire lengths, suggesting recent transfer of the phage among divergent bacterial host species (Figure S3). The remaining members, *Tannerella* sp. 6_1_58_FAA_CT1 and *B. coprophilus* DSM 18228, exhibit large 48-kb and 19-kb replacements, respectively, as well as a large 69-kb deletion in *B. coprophilus* DSM 18228, suggesting that one or both of these are inactivated prophage (Figure S3). Although the MCL clustering grouped *B. finegoldii* and *B. stercoris* into Family 2, this relationship is largely driven by their extended homology surrounding the *btu* locus (Figure S4). It is likely that with further investigation and identification of corrinoid transport-encoding CTns, this family may be subdivided. It is notable that extended homology (43 kb) is observed surrounding the *btu* locus between *B. thetaiotaomicron* VPI-5482 chromosomally encoded *btu* Locus 2 and the *btu* locus in the *B. stercoris* predicted MGE (Figure S4). This further supports the role of HGT and CTns in the distribution *btu* alleles in diverse gut microbes (Degnan et al., 2014b).

Family 1 corrinoid transport-encoding CTns are mobilizable and transport vitamin B_{12}

Conjugation experiments were carried out with two MGE Family 1 representative strains, *B. ovatus* ATCC 8483 (*B. ovatus*) and *B. thetaiotaomicron* 7330 to determine if these predicted elements are capable of transferring via conjugation. These CTn-containing strains acted as donors, and an erythromycin-resistant triple corrinoid transport locus mutant of *B. thetaiotaomicron* as the recipient (*B. thetaiotaomicron* ΔΔΔ Erm^R, Table 2). In minimal medium supplemented with vitamin B_{12} (minimal medium [MM] + B_{12}), *B. thetaiotaomicron* ΔΔΔ is a methionine auxotroph, as it can no longer import corrinoids (Degnan et al., 2014b; Varel and Bryant, 1974). Therefore, successful transconjugants, but not original recipients or donors, will grow on MM + B_{12} + Erm. This is in fact what we observed, isolating putative transconjugants derived from both *B. ovatus* and *B. thetaiotaomicron* 7330 predicted CTn-encoding donor strains (Figure 2A, Table S4).

Conjugation frequencies for both strains were calculated by taking the average of the transconjugant (MM + B_{12}) CFUs divided by the CFUs of the transconjugants and recipients (MM + Met) from each experiment. We found that the transfer frequency of the BtCTn (1.02×10^{-5}) was nearly three times greater than that of the BoCTn (2.83×10^{-5}) (Figure 2A, Table S4).

To determine if the isolated transconjugants from the initial experiment (*B. thetaiotaomicron* ΔΔΔ Erm^R + BoCTn or BtCTn) encoded the entirety of the required transfer machinery, these strains were used as donors and *B. thetaiotaomicron* ΔΔΔ Tet^R as the recipient in a second round of conjugation experiments. We obtained successful secondary transconjugants for both CTns, indicating the acquisition of all the necessary transfer machinery by the initial transconjugants (Figure 2B, Table S4). Notably, in the second round of transfers, the CTn transfer frequency of the BoCTn was ~16-times greater than the transfer frequency of the BoCTn from its original host, whereas the secondary transfer frequency of the BtCTn was about the same as the original. Correspondingly, the transfer frequency of the BoCTn from the new transconjugants to *B. thetaiotaomicron* ΔΔΔ Tet^R was ~42-times greater than that of the BtCTn (Figure 2B, Table S4).

Although transconjugants were isolated on MM + B_{12} plates, we confirmed the ability of the corrinoid transport locus on the CTn to be expressed, translated, and functional for importing vitamin B_{12} in their new hosts by assessing growth rate of donors, recipients, and representative transconjugants in MM + B_{12} and MM + Met. Transconjugants were found to grow at similar rates as the donors in both media types and the original *B. thetaiotaomicron* ΔΔΔ recipients only grew when methionine was supplemented (Figure 2C).

Many Bacteroidetes CTns have relatively broad host ranges (Bertram et al., 1991; Salyers and Shoemaker, 1994; Trieu-Cuot et al., 1988). To test this, we introduced a Tet^R cassette into BoCTn and BtCTns and attempted conjugations with several Tet^S recipient gut microbes. Overall, we found that the BoCTn and BtCTns were able to transfer to *B. uniformis* ATCC 8492 and *B. vulgatus* ATCC 8482 strains but not *B. fragilis* NCTC 9343 and *B. caccae* ATCC 43185 (Table S4). There could be a variety of factors inhibiting the transfer of the CTns to *B. fragilis* and *B. caccae,* including CRISPR systems, restriction modification systems, masking or occupation of the attachment site, culture conditions, etc. that remain to be explored.

BoCTn and BtCTn have conserved conjugation and integration mechanisms

As an initial confirmation of CTn insertion, pulsed-field gel electrophoresis (PFGE) and Southern hybridizations were performed. PFGE of recipients, donors, and representative transconjugants clearly revealed an additional band in the transconjugants as compared with the recipient strain (Figure 3A). Southern hybridizations of the gels using a biotinylated probe specific for the outer membrane corrinoid transporter, *btuB,* consistently found that the extra bands in the gel hybridized with the *btuB*-specific probe (Figure 3B). In the majority of cases, the additional, *btuB*-containing band appeared in the same location on the gel for both the BoCTn and BtCTn (~100 kb), raising the possibility that these CTns use the same attachment site. In a small number of cases (7 of 32), the additional band appeared at a different molecular size or two additional bands were observed, raising the possibility

of a second attachment site and/or multiple integrations (see *B. ovatus* transconjugant 1 in Figures 3A and 3B).

Whole genome sequencing was performed on 11 representative transconjugants encoding the BoCTn and 11 encoding the BtCTn (Table S5). These sequences were used to confirm and refine the initial predictions. Pairwise comparison of BoCTn and BtCTn indicate that these CTns share a common ~80-kb backbone but encode several variable regions (Figure 3C). As part of their conserved backbone, the CTns share integrase, mobilization, and transfer genes that are 99% to 100% conserved at the amino acid level (Figure 3C). Despite both the BoCTn and BtCTn BtuB alleles nesting within the same phylogenetic clade (Figure 1A), the BtuGBFCD proteins are on average only 95% similar to one another and encode varied gene content immediately up- and downstream. An analysis of conserved protein domains in the variable CTn regions identified one unique TIGRFAM (in BoCTn) and 31 unique PFAMs, 26 of which were detected in BtCTn, which is 16 kb longer than the BoCTn (Table S6). The additional DNA in BtCTn includes a mobilizable restriction modification system integron (12 kb) and an operon possibly involved in lipid transport and methylation (6 kb) (Tables S5 and S6). BoCTn encodes a putative threonine/serine exporter downstream of its *btuGBFCD* operon and several additional genes of unknown function (Table S6).

To determine an attachment site (*attB*) for the CTns, the CTn boundaries within the sequenced contigs were aligned with the recipient *B. thetaiotaomicron* strain using Mauve (Darling et al., 2004). This identified 18 nucleotide *attL* and *attR* direct repeat sequences that were nearly identical to the putative *attB* in *B. thetaiotaomicron* (ACTAAATTTACCAGATTT, Figure S5). Confirmation of integration of the CTns at the main *attB* in the intergenic spacer between *BT4140* and *BT4141* was attempted in 153 of 289 transconjugants via a negative PCR across the main attachment site (*attB*). Integration at this site was PCR confirmed in 118 of the 153 tested. Four of the genome-sequenced transconjugants were determined to have integrated in different locations in the *B. thetaiotaomicron* chromosome. Two were identified between *BT2505* and *BT2506*, and one each within *BT4088* and *BT4227* (Table S5). These alternate attachment sites differed by 3, 3, and 5 base pairs (bp), respectively, from the primary *attB*, mostly clustered near the 5′ end of the sequence (Figure S5), indicating some flexibility in the integrase recognition site specificity. We then examined the remaining Family 1 MGEs for evidence of homologous *attL* and *attR* sites given they encode nearly identical integrases (97%–100% amino acid identity). This revealed that nearly all Family 1 MGEs encode attachment site sequences that are nearly identical to the attachment sites identified in the BoCTn and BtCTn transconjugants with limited nucleotide differences occurring near the 5′ end of some of the *attL* sequences (Figure S5). However, even with a high degree of conservation of the *attL/attR* sites among the Family 1 MGEs, there is not conservation in the genomic context that these MGEs integrate within. This differs from what is seen with some other MGEs where integration of the element occurs near a tRNA (Burrus et al., 2002). Regardless, possible *att* sites were detected in the majority of Bacteroidetes genomes analyzed (1 mismatch allowed, 112 of 133 genomes). As expected, the Family 2 and Family 3 corrinoid transport MGEs, as well as the Family 1 *B. plebeius* MGE, encode divergent integrases and all encode correspondingly distinct predicted attachment sites (Figure 1B; Tables 1 and S1).

CTn-encoded corrinoid transport loci provide distinct competitive advantages

Previous work on chromosomally encoded corrinoid transport loci within *B. thetaiotaomicron* revealed that, despite sequence and structural homology, each of the three corrinoid transport loci in *B. thetaiotaomicron* have distinct corrinoid preferences (Degnan et al., 2014b). These preferences occur even between BtuB2 and BtuB3, which are 73% identical at the amino acid level. Of the three chromosomal corrinoid transport loci, Locus 2, encoding BtuB2, is the most competitively advantageous both *in vitro* as well as in a mouse model (Degnan et al., 2014b). Therefore, similar competition assays were carried out to determine the relative fitness of strains encoding the corrinoid transport-encoding CTns compared with the chromosomally encoded corrinoid transport alleles.

B. thetaiotaomicron corrinoid transport mutant strains encoding the BoCTn, BtCTn, or individual chromosomal corrinoid transport loci were marked with unique oligonucleotide barcodes and competed (Table 2, Figure 4) (Martens et al., 2008). *In vitro* competitions were carried out as in Degnan et al. (2014b) comparing growth of strains over 5 days of serial transfer in both competitive (MM + B_{12}) and control conditions (MM + Met). As expected, when the CTn-containing strains were competed against the triple-locus deletion, *B. thetaiotaomicron* ΔΔΔ BC, both CTn-containing strains completely outcompeted this strain defective in vitamin B_{12} transport in competitive but not control conditions (Figures 4 and S6). However, the competitive abilities of the CTn-containing strains when paired head-to-head with the individual chromosomal corrinoid transport loci were not as predictable. We determined that both CTn-containing strains were outcompeted by both the Locus 1 and Locus 2 corrinoid transport loci. Although we note that strains with the BoCTn are greatly outcompeted by *B. thetaiotaomicron* Δ*locus1*Δ*locus3* BC (99:1), while strains with the BtCTn are closer to a 50:50 ratio (Figure 4). In contrast, both the *B. thetaiotaomicron* ΔΔΔ + BoCTn BC and *B. thetaiotaomicron* ΔΔΔ + BtCTn BC strains greatly outcompete *B. thetaiotaomicron* Δ*locus1*Δ*locus2* BC, which only has the chromosomal Locus 3 intact (Figure 4). Competitive performance of the CTn strains in the control medium was variable with strains containing the BoCTn being outcompeted, regardless of which chromosomal corrinoid transport locus mutant they were competed against while strains containing the BtCTn greatly outcompeted *B. thetaiotaomicron Δlocus1 Δlocus3* BC strains, were about equal with *B. thetaiotaomicron* Δ*BT1953*Δ*BT2094* BC strains, and were outcompeted by *B. thetaiotaomicron* Δ*locus1* Δ*locus2* BC strains (Figure S6).

The competitive differences between the CTn and chromosomally encoded loci cannot be wholly explained by differences in individual growth rates, as barcoded strains were assessed for their ability to grow in both the competitive and control media and no significant growth defects were identified (Figure S6C). We note that CTn transfer during the competition would have an effect on the interpretation of these results; however, this possibility was assessed by attempting liquid- versus solid-phase conjugation assays. As reported elsewhere, CTn transfer requires cell-to-cell contact (Alvarez-Martinez and Christie, 2009; Johnson and Grossman, 2016; Scott, 2002; Stecher et al., 2012), and we found it exceedingly rare (~10^{-8}) in liquid cultures and therefore it is unlikely that transfer of the CTns was occurring in the course of these competitions.

Although successful conjugation is rare, CTns are still able to excise and re-integrate into the chromosome when cultured in liquid medium. Using qPCR, we determined that the relative quantity of the integrated and excised forms of BtCTn and BoCTn are not different during mid-log growth in competitive (MM + B_{12}) and control conditions (MM + Met) (Figures S6D and S6E). We did find that the excised BtCTn copy number is ~1.8 times greater than BoCTn (Figures S6F and S6G) but it is unclear if this has any influence on the major competitive differences observed with the *B. thetaiotaomicron Δlocus1 Δlocus3* BC strain (Figure 4).

BoCTn and BtCTn mobilize in the mammalian intestinal tract

MGE transfer is widespread within the gut, suggesting that the gut acts more as a structured environment and less like a liquid culture (Coyne et al., 2014; Zhao et al., 2019). Therefore, we endeavored to determine if the BoCTn and BtCTn corrinoid transport-encoding elements could mobilize *in vivo*. To this end, we pre-colonized Germ-free mice with excess of the recipient *B. thetaiotaomicron* ΔΔΔ Erm^R strain, which is normally outcompeted by strains competent in corrinoid transport. We then gavaged the mice with equal portions of donor strains *B. thetaiotaomicron* ΔΔΔ + BoCTn_Tet^R and *B. thetaiotaomicron* ΔΔΔ + BtCTn_Tet^R and plated fecal pellets to detect transconjugants (Erm^R + Tet^R). After 3 days, no transconjugants (recipient cells (Erm^R)) that had gained a Tet^R marked CTn (BoCTn_Tet^R or BtCTn_Tet^R) were observed (Figure 5). We next hypothesized that MGE transfer occurs in a density-dependent fashion within the gut, with the initial inoculum of ~3.2×10^5 colony-forming units (CFUs) for the donor cells being too low to support element transfer, especially as the level of donor cells dropped to ~2.6×10^2 on days 1 to 3 (Figure 5). This drop in the donor population suggests that despite the fact that *B. thetaiotaomicron* ΔΔΔ Erm^R lacks functional corrinoid transport, the initial establishment of this strain within the host likely provided it with colonization resistance (Litvak and Bäumler, 2019). Therefore, on day 4, the mice were gavaged a second time with ~3.2×10^{10} CFUs of equal portions of the two donor strains.

Immediately following the second gavage, transconjugants encoding either the BoCTn or BtCTn were isolated from the mouse gut (Figure 5). Once detected, the abundance of the transconjugants remained fairly steady, showing a slight increase over the course of the experiment. The total transfer frequencies for these CTns *in vivo* ranged from ~9.7×10^{-9} on day 5 to the highest on day 9 of ~1.0×10^{-7} (Figure 5). However, calculating precise transfer frequencies is complicated by the presence of both BoCTn and BtCTn transconjugants and the inability to distinguish unique transconjugant events from the maintenance of already established transconjugants. We note that these *in vivo* conjugation rates are much lower than those observed for the BoCTn and BtCTn *in vitro* (Figures 2A and 2B). As efficient conjugative transfer heavily relies on physical contact, it is possible that the structured gut environment, gastric motility, the host immune system, or other factors may have contributed to the lower transfer rates observed (Alvarez-Martinez and Christie, 2009; Johnson and Grossman, 2016; Scott, 2002; Stecher et al., 2012). We expect that new transconjugants have equal fitness with the donor strains. Therefore, given the 10-fold increase in transconjugants and donors during the final 7 days of the experiment, if

continued we would predict the corrinoid transport-deficient recipients would eventually be replaced by donors and transconjugants.

Following isolation, a total of 92 transconjugants from days 5, 7, 9, and 12 were confirmed by PCR for the presence of BoCTn (n = 59) or BtCTn (n = 33) and the site-specific Erm^R insertion. A subset of 24 of these isolates were further confirmed for successful growth in MM + B_{12} (Figure S7). These results demonstrate that these predicted corrinoid transport-encoding CTns are functional in both transfer and restoration of growth on corrinoid species *in vivo*. Furthermore, this suggests that these elements play a key role in re-assorting corrinoid transporters and influencing competition and colonization in the mammalian gut.

DISCUSSION

The human gut microbiome is incredibly important to human health, and its functional diversity is shaped by MGEs. While many characterized MGEs increase their host's fitness through the spread of antibiotic resistance (Bacic et al., 2005; Gupta et al., 2003; Salyers et al., 2004; Shoemaker et al., 2001; Tribble et al., 1999; Wang et al., 2000, 2004; Welch et al., 1979; Wesslund et al., 2007) and antagonistic type 6 secretion systems (Coyne et al., 2014, 2016), any gene that is beneficial to a host's survival and colonization should facilitate the spread of an MGE within a population (Rankin et al., 2011; Top and Springael, 2003). In this study, we identified 19 putative MGEs integrated into human gut Bacteroidetes genomes that encode putative corrinoid transport loci homologous to those we previously described in *B. thetaiotaomicron* VPI-5482 that are critical for colonization and competition in the mammalian gut (Table 1)(Degnan et al., 2014b; Goodman et al., 2009). We were able to classify these MGEs into three distinct families, two that are composed of CTns and the third that is putative phage (Figure 1). Furthermore, we were able to demonstrate the ability of two of the CTns to mobilize and functionally complement vitamin B_{12} transport (Figure 2). Finally, conjugation was also detected by both CTns during colonization of a gnotobiotic mouse model, confirming the role of these MGEs in disseminating corrinoid transporters and influencing competition and colonization in the mammalian gut (Figure 5).

Corrinoids are required small molecule cofactors for the majority of sequenced gut microbes (Degnan et al., 2014b; Zhang et al., 2009). While some gut microbes are capable of synthesizing these cofactors *de novo*, a large proportion rely on transporters to access these critical molecules (Degnan et al., 2014b). Our previous analysis of corrinoid transport gene clusters among diverse Bacteroidetes led us to speculate that part of the diversity and distribution of these loci was due to HGT among these species (Degnan et al., 2014b). In examining the genetic context of the 33 Family N BtuB alleles previously identified, we found that 11 were closely flanked by genes with strong homology to CTn and phage protein domains. Subsequent comparisons with additional gut microbial genomes led to the refinement of the MGE boundaries and identified eight more predicted MGEs encoding additional Family N BtuB alleles. Like the previously reported chromosomal loci, all of the MGE-encoded BtuBs were localized in operons preceded by a B_{12} binding riboswitch and encoding the additional transport proteins BtuGFCD (Degnan et al., 2014b; Wexler et al., 2018).

Despite the similarity of the corrinoid transport loci, the MGEs encoding these loci were readily resolved into three distinct families (Figure 1). Given the abundance and importance of CTns in Bacteroidetes genomes, the identification of two CTn families responsible for mobilizing corrinoid transport loci was not surprising (Coyne et al., 2014; Quesada-Gómez, 2011; Shoemaker et al., 2001; Whittle et al., 2002). In contrast, the identification of a group of integrated prophage with corrinoid transport loci was at first unexpected; however, is consistent with the ability of phage to encode genes that can directly contribute to their bacterial host's fitness (e.g., Shiga toxin, cholera toxin) (O'Brien et al., 1984; Waldor and Mekalanos, 1996). We note that these MGEs are distributed among diverse species and strains isolated from a combination of both healthy and sick patients (e.g., ulcerative colitis, Crohn's disease) dating between 1933 and 2014 from the United States, Canada, and Japan (Table S1). This suggests the broad circulation and maintenance of these MGE families among human gut Bacteroidetes communities.

Alignments of Family 1 and Family 3 MGEs show broad synteny within these integrated element families (Figures S2 and S3) while this synteny is considerably less in alignments of Family 2 MGEs (Figure S4). In Family 1, the synteny is disrupted in several cases by an isolated Group II intron insertion or an insertion sequence element. Furthermore, we detected four distinct putative restriction modification gene integrons, all of which are flanked by integrase family genes, suggesting their independent acquisitions by these CTns. For example, in the case of the sequenced BtCTn transconjugants, five of the 11 isolates spontaneously lost this integron (Table S5). In Family 3, three virtually identical phages were detected in three distinct *Bacteroides* species; however, all were isolated from separate patient biopsy samples collected in Calgary, Alberta, Canada. A fourth representative found in a *Tannerella* species, also from a patient sample from the same research group, has an apparent non-orthologous replacement of 47 kb of phage DNA (Figure S3). This type of mosaicism is common among phage and can result in phage structural changes and/or permit infection of novel hosts (Casjens et al., 2004; Clark et al., 2001; Juhala et al., 2000). Of the 19 corrinoid transport-encoding MGEs we identified in this study, only the final member of Family 3 has clear evidence of substantial genetic loss and rearrangement that would suggest it is no longer an active phage. However, bioinformatics alone cannot rule out the possibility that genomic regions are mobilizable, given the presence of helper phage or CTns (Carpena et al., 2016; Duerkop et al., 2012).

We experimentally characterized two of the predicted Family 1 CTns, confirming their ability to independently transfer to and from *B. thetaiotaomicron* both *in vitro* as well as in a gnotobiotic animal model (Figures 2, 3, and 5). Furthermore, we demonstrated that the CTn-encoded corrinoid transporters were capable of functionally complementing strains otherwise incapable of transporting vitamin B_{12} (Figure 2C). Similar to our previous observations (Degnan et al., 2014b), although the BoCTn- and BtCTn-encoded BtuB fall in the same corrinoid transporter Family (Family N) as two of the chromosomally encoded transporters in *B. thetaiotaomicron* VPI-5482, they exhibit distinct competitive abilities in acquiring vitamin B_{12} (Figure 4). Indeed, the acquisition of BoCTn or BtCTn by a gut microbe only encoding a *btuGBFCD* operon like chromosomal Locus 3 would presumably provide it with a marked fitness improvement. Future experiments are still required to assess both if there are distinct preferences among the CTn-encoded transporters for other

corrinoids and what factors (e.g., binding affinities, expression levels) contribute to these preferences.

Consistent with the diversity of hosts initially identified harboring a Family 1 CTn, we demonstrated that both BoCTn and BtCTn were capable of transferring to divergent *Bacteroides* species (*B. uniformis* and *B. vulgatus*) (Table S4). We note that we were not able to detect transconjugants in all of the species tested (*B. fragilis* and *B. caccae*); however, there are likely a multitude of factors that could interfere with successful conjugation of these elements. For example, we have previously shown that gut colonization was critical for detecting transduction of the *Bacteroides* phage, BV01 (Campbell et al., 2020). We find it likely that conjugation frequency and compatibility may also be modulated by growth in the intestinal environment. In addition, we saw a marked increase in BoCTn transfer frequency during the secondary round of transfer when this MGE was transferring among *B. thetaiotaomicron* species as compared with when the MGE was transferring from its original *B. ovatus* host to *B. thetaiotaomicron* (Figures 2A and 2B, Table S4). This potentially indicates a slight species barrier that leads to a lower transfer frequency between more distantly related organisms. Interestingly, six of the 12 members of Family 1 appear to have integrated either within or immediately adjacent to another mobile-like region (Figure S2). Although nearly all of the Family 1 MGEs share a conserved attachment site (Figure S5), it is clear that genomic locations of these attachment sites are not conserved. Furthermore, it is unclear what effect, if any, the integration of the Family 1 CTn has on the activity of the nearby element. It is possible that the function of the nearby element is disturbed or that the elements are now capable of transferring as a single conjugative element.

In stark contrast to many of the characterized MGEs encoded by the Bacteroidetes, the MGEs identified in this study do not carry a tetracycline resistance gene, or any genes homologous to any known antibiotic resistance genes, and have limited similarity to CTnDOT (Bacic et al., 2005; Buckwold et al., 2007; Gupta et al., 2003; Wang et al., 2000, 2011). These antibiotic resistance MGEs within the Bacteroidetes spread as a result of the widespread clinical use of tetracycline in the 1980s and 1990s (Shoemaker et al., 2001). The MGEs in this study represent a different class of MGEs that do not contain antibiotic resistance cassettes, but rather loci that allow the host to gain or increase access to an essential metabolite (Coyne et al., 2014). They are akin to the integrative and conjugative elements encoding polysaccharide utilization loci, one of which that is responsible for catabolizing algal polysaccharides and is common among individuals in Japan that regularly consume seaweed products (Hehemann et al., 2012). The success and spread of these MGEs in populations is expected if the corrinoid transporter expands the corrinoid repertoire of the host or encodes a more effective transporter, thereby increasing fitness of the host.

Together, this work has identified a distinct class of MGEs that encode corrinoid transporters and are widespread among gut Bacteroidetes. For these gut Bacteroidetes, the presence of corrinoid transporters is crucial, as many are unable to synthesize this essential cofactor. Therefore, these MGE-encoded transporters have the potential to expand the corrinoid repertoire of their host, leading to a competitive advantage in the human gut where the ability to transport corrinoids has been shown to be essential for colonization. Future

investigations into how MGEs contribute to the spread, maintenance, and distribution of corrinoid transporters among the Bacteroidetes are essential, as they provide insight to novel factors that affect colonization, and thus composition, of the human gut microbiome.

STAR★METHODS

RESOURCE AVAILABILITY

Lead contact—Further information and requests for resources and reagents should be directed to and will be fulfilled by the lead contact, Dr. Patrick Degnan (patrick.degnan@ucr.edu).

Materials availability—Bacterial strains and plasmids generated in this study are available upon request to the lead contact, Dr. Patrick Degnan (patrick.degnan@ucr.edu).

Data and code availability—All NCBI Accession numbers for genomes used and sequenced in this study can be found in Table S2. DNA sequencing reads from the transconjugants generated in this study are deposited in NCBI under BioProject: PRJNA715234. Information regarding these sequences can be found in Table S5. New assembled genomes are also deposited in NCBI under BioProject: PRJNA715234. The code used for the genome assembly is available here https://github.com/phdegnan/A5ud (https://doi.org/10.5281/zenodo.5712008). The code for the generation of pairwise percent length alignment (PLA) and reformatting these files for Markov Cluster algorithm analysis can be found here https://github.com/IGBIllinois/VICSIN (https://doi.org/10.5281/zenodo.5138177). Any additional information required to reanalyze the data reported in this paper is available from the lead contact upon request.

EXPERIMENTAL MODEL AND SUBJECT DETAILS

Bacterial culturing and genetic manipulation—Bacterial strains used in this work can be found in Tables 2 and S7. Routine culturing of *Bacteroides* species occurred anaerobically at 37°C in liquid tryptone-yeast extract-glucose (TYG (Holdeman et al., 1977)) medium or Difco Brain Heart Infusion (BHI, Quad Five, Ryegate, MT) agar with the addition of 10% defibrinated horse blood as previously described (Costliow and Degnan, 2017). Anaerobic culturing was performed in a vinyl anaerobic chamber containing a 70% N_2, 20% CO_2, and 10% H_2 gas mixture (Coy Laboratory Products, Grass Lake, MI). *Escherichia coli* S17-1 lambda pir strains used for cloning and conjugation of suicide vectors were grown in Lysogeny Broth (LB) at 37°C aerobically with shaking (Campbell et al., 2020; Costliow and Degnan, 2017; Degnan et al., 2014b). When needed, cultures were resuspended or grown in minimal medium (MM (Degnan et al., 2014b; Martens et al., 2008)). As noted, MM was supplemented with methionine (MM + Met, 500 μM) or vitamin B_{12} (MM + B_{12}, 0.4 or 4 nM) and agar (20 g/L) was added for plate preparation as needed. Antibiotics were added to the medium when appropriate in the following concentrations: ampicillin, 100 μg/mL; gentamicin, 200 μg/mL; erythromycin, 25 μg/mL; tetracycline, 2 μg/mL; and 5-fluoro-2'-deoxyuridine (FudR), 200 μg/mL.

All vectors and primers used in this study can be found in Table S7, with vector sequences found as Data S1. Insertion of the *tetQ* allele into BoCTn and BtCTn was accomplished via allelic exchange conjugated from donor *E. coli* S17-1 lambda pir strains into recipient *B. thetaiotaomicron* strains before being confirmed by PCR (Costliow and Degnan, 2017; Degnan et al., 2014b; Koropatkin et al., 2008). Briefly, the ~1kb left and right flanks of the MGE regions surrounding *BACOVA4685* (BoCTn) or *Bthe2347* (BtCTn) were amplified via HiFi PCR (Kapa HiFi Taq MasterMix, Kapa Biosystems, Wilmington, MA) and combined by splicing overlap extension (SOE) PCR designed to insert BamHI and SpeI restriction sites in the middle of the region. The *tetQ* allele was also amplified via HiFi PCR. The purified SOE products and *tetQ* were digested with restriction enzymes, cloned into pExchange_tdk vector, and transconjugants screened by standard methods (Campbell et al., 2020; Costliow and Degnan, 2017; Koropatkin et al., 2008; Martens et al., 2008). Barcoded pNBU2 vectors were constructed previously and were introduced into the genome in a single copy using methods similar to pExchange_tdk (Costliow and Degnan, 2017; Koropatkin et al., 2008).

Gnotobiotic mice—All experiments using mice were performed using protocols approved by the University of California Riverside Institutional Animal Care and Use Committee. Germfree C57BL/6J mice were maintained in flexible plastic gnotobiotic isolators with a 12-h light/dark cycle. Animals caged individually (n = 1, female) or in pairs of littermates (n = 2 males, n = 2 females) were provided with standard, autoclaved mouse chow (5K67 LabDiet, Purina) *ad libitum*. Since there was no *a priori* reason to expect animal age to influence conjugation rates, animals were 11 week old at time of colonization. Individually antibiotic resistance marked bacterial strains were grown individually for ~20h in TYG medium with appropriate antibiotics and frozen at −80°C in anaerobic cryovials. Cell viability was tested by plating. Viable CFU counts were used to prep the recipient cells *B. thetaiotaomicron* ΔΔΔ Erm^R for oral gavage on Day −2 at ~3.2×10^6 CFUs per animal. On Day 0, equal amounts of two donor strains *B. thetaiotaomicron* ΔΔΔ + BoCTn_Tet^R and *B. thetaiotaomicron* ΔΔΔ + BtCTn_Tet^R were combined and gavaged at ~3.2×10^5 CFUs. A second gavage of equal amounts of the two donor strains were given on Day 4 at a concentration of ~3.2×10^{10} CFUs per animal. Fecal samples were collected on days 0 prior to gavage of the donors followed by days 1, 3, 5, 7, 9, and 12 from each animal. Fecal pellets were processed by adding 500 μL of TYG +20% vol/vol glycerol to each tube and vigorously shaking in a beadbeater without beads for 1m 30s. Fecal slurries were spun down at 2,000 × g for 10s, followed by serial dilution on selective media (BHI + Tet + Gn, BHI + Erm + Gn, BHI + Erm + Tet + Gn) to determine CFUs. Animals were sacrificed on day 12 following final fecal collection. A maximum of 5 individual isolates per animal were struck out on BHI + Erm + Tet + Gn media, before being stocked at −80°C and prepped for gDNA and PCR screening. Isolates predicted to be successful transconjugants were screened as above (screening of isolates, and Liquid Growth Assays).

METHOD DETAILS

Identification of predicted MGEs—Bacteroidetes genomes (Table S2) were screened for the presence of genomic regions encoding mobile-like genes using HMMER v3 (hmmer.org) with trusted cutoffs (–cut_tc) for PFAMs (El-Gebali et al., 2019) and

TIGRFAMs (Haft, 2001)(Table S3). Boundaries for the predicted mobile regions were identified using a combination of BLASTn and Mauve (Darling et al., 2004) to compare strains containing the predicted element to those of the same, or closely related, species without the element. Predicted attachment sites (*attL* and *attR*) for the elements were determined by examination of alignments of the element boundaries for short, repeated sequences. Additionally, once attachment sites were determined for the BoCTn and BtCTn transconjugants sequenced in this study, Fuzznuc (Rice et al., 2000) was utilized to search for similar attachment sites in other Bacteroidetes genomes.

Relationships and relatedness of predicted MGEs—MGE-encoded BtuB alleles were initially detected by BLASTp using BtuB1, BtuB2, and BtuB3 from *B. thetaiotaomicron* VPI-5482 as queries. These BtuB alleles were then aligned with a subset of those detected previously (Degnan et al., 2014b) using MUSCLE (Edgar, 2004) and subjected to maximum likelihood based phylogenetic reconstruction with RAxML on the CIPRES server (Miller et al., 2010; Stamatakis, 2006). BLASTp was also used to calculate protein similarity among the MGE-encoded integrases (e-value cutoff of 0.1).

Nucleotide sequences for each predicted MGE were aligned using Mauve (Darling et al., 2004) and compared pairwise using BLASTn with an e-value cutoff of 0.0001. These results were analyzed to calculate the percent length aligned (PLA), total length aligned, and total bit score for each pair using Blast_to_MCL.1.py. PLA values below 0.2 were excluded and the Markov Cluster algorithm (MCL algorithm) was used to generate a relatedness network and family groupings of the predicted MGEs using MCLdump2clusters.py (Enright, 2002; van Dongen 2000). The network was visualized in Cytoscape (Shannon, 2003).

Conjugation/screening of isolates with Bo/BtCTn—Cells were grown in TYG to exponential phase (0.3 – 0.6 $O.D._{600}$) and then pelleted and washed in PBS. Donor and recipient strains were then combined in PBS before plating on BHI agar + 10% horse blood for 16 hours. Cell lawn was then resuspended in PBS and washed four times in MM. Cells were then plated on selective media (BHI + Ab (Erm or Tet) + Gent, MM+Met + Ab (Erm or Tet) + Gent, and MM+B_{12} (4nM) + Ab (Erm or Tet) + Gent) and grown anaerobically for 16 – 72 hours.

Colonies that were isolated from conjugations after plating on selective media were then screened to confirm they were transconjugants. Cells were confirmed for their ability to grow on selective media (Erm^R or Tet^R depending on the identity of the recipient strain), the presence of a *btuB* in their genome (as detected by PCR, Primers in Table S7), the correct sequence of the *btuB* in their genome (confirmed by Sanger Sequencing), and their ability to grow in MM+B_{12}.

Liquid growth assays—Cells were grown in TYG to stationary phase and then pelleted and washed four times in MM (Degnan et al., 2014b). Cells were then normalized, and cultures were inoculated in a 96-well plate in triplicate at 0.003 $O.D._{600}$ in TYG, MM+Met, and MM+B_{12} (4nM). When performing the growth assays comparing barcoded and non-barcoded strains (Figure S6C) growth was also assessed in MM+B_{12} (0.4nM). Growth was then monitored every 30 minutes for 36 hours using a BioTek Synergy HTX Multi-Mode

microplate reader in conjunction with a BioStack3 microplate stacker (BioTek, Winooski, VT, (Costliow and Degnan, 2017)) or on a Clariostar microplate reader with a Stack III microplate stacker (BMG Labtech, Cary, NY). Doubling times were calculated from cells in early to mid-log phase ($O.D._{600}$ of 0.01 – 0.12) using the least-squares fitting method (http://www.doubling-time.com/compute.php?lang=en).

PFGE and Southern hybridizations—Whole-cell agarose plugs were made from overnight stationary cultures. Cultures were harvested and resuspended in TE Buffer (10 mM Tris, 1 mM EDTA, pH 8.0) before being combined 1:1 with 1.5% InCERT/LMP agarose. Once set, plugs were digested with Proteinase K (20mg/mL) before being washed and stored at 4°C in Low TE Buffer (10 mM Tris, 0.1 mM EDTA, pH 8.0) (Degnan and Moran, 2008). Plugs were then digested with NotI before being run on a pulsed field gel electrophoresis (PFGE) rig for 24 hours to resolve bands 50 to −1000 kb. Conditions were as follows: 1% PFGE agarose; initial switch time, 24 seconds; final switch time, 2 min 30 seconds; Buffer, 0.5x Tris-borate-EDTA (TBE); V/cm, 6.0. Yeast Chromosomal PFG-Marker Mid-Range ladder was included for band size comparison (NEB). After the gel was visualized, the DNA was transferred overnight to a nitrocellulose membrane then probed overnight with a biotinylated, universal *btuB* specific probe at 42°C (Table S7). Detection was performed per manufacturer's protocol (Chemiluminescent Nucleic Acid Detection Module Kit, Thermo Fisher Scientific) using autoradiography film.

Whole genome sequencing—Twenty two representative transconjugant strains from eight independent conjugation experiments were selected for sequencing. In addition, 13 historical *Bacteroides* strains from the Virginia Polytechnic Institute Anaerobe Laboratory (VPI) and Wadsworth Anaerobe Laboratory (WAL) strain collections were sequenced. Sequencing was done as performed previously (Campbell et al., 2020). Briefly, total high molecular weight gDNA was extracted as performed previously (Campbell et al., 2020). This inovles resuspension of overnight cell pellets in TE buffer (10mM Tris, 1mM EDTA) followed by lysis with sodium dodecyl sulfate (SDS; 0.07% w/v final) and proteinase K (300μg/mL final) and incubation at 55°C for 2 h. Lysates were then mixed and centrifuged twice with phenol:chloroform:iso-amyl alcohol (25:24:1) (v/v/v), and the aqueous phase was retained and precipitated with 2 volumes of 100% EtOH and $1/10^{th}$ volume of 0.3M sodium acetate at −20°C. DNA was pelleted with centrifugation at max speed for 30 min, then washed with 70% EtOH, dried and resuspended in TE buffer. DNA libraries were prepped with the Nextera XT Library Preparation Kit and Index Kit (Illumina, San Diego, CA), and the samples were pooled and submitted for sequencing on a HiSeq 2500 or HiSeq 5000 Illumina sequencer. Genomes were then assembled as performed previously (Campbell et al., 2020) and mapped back to a *B. thetaiotaomicron* reference genome, as well as the genomic regions of *B. thetaiotaomicron* 7330 or *B. ovatus* encoding the CTn using BRESEQ v0.33.2 (Deatherage and Barrick 2014).

***In vitro* competition assays—**Competitions between strains carrying unique oligonucleotide barcodes were performed as described previously (Costliow and Degnan, 2017; Degnan et al., 2014b). Briefly, barcoded cells were grown for 16 h in TYG then pelleted and washed four times with MM. $O.D._{600}$ values were normalized to 0.4 before

being combined at a 1:1 ratio and inoculated 1:1,000 into an Axygen deep-well plate (Corning, Inc., Corning, NY) in triplicate for each conjugation pair in MM + Met and MM + B_{12} (0.4nM). Cultures were incubated anaerobically at 37°C for 24 h and passaged 1:1,000 into the same medium they were previously grown in (Costliow and Degnan, 2017; Degnan et al., 2014b; Koropatkin et al., 2008). Time points were taken every 24 h and samples were saved in medium plus 20% glycerol at −80°C in 96-well plates. Samples were prepared and analyzed using qPCR as previously described (Bookout et al., 2006; Costliow and Degnan, 2017) on a Bio-Rad CFX Connect instrument (Bio-Rad, Hercules, CA) with SYBR Fast MasterMix 2X Universal (Kapa Biosystems, Wilmington, MA). Briefly, this employed the HotSHOT 96-well plate method (Truett et al., 2000), which lyses 5 μL of cultured cells in 50 μL of the lysis buffer (25 mM NaOH, 0.2 mM EDTA) during a 30 min incubation at 95°C. A fraction of the lysate (16 μL) is then combined with 144 μL of 10 mM Tris pH 8.0 and 16 μL of neutralization buffer (40 mM Tris-HCl). Each sample was run in technical triplicate using the manufacturer's instructions for the SYBR Fast Master Mix for reach relevant set of barcode primers. A single touchdown PCR protocol was previously optimized (Degnan et al., 2014b) and used on the Bio-Rad CFX Connect instrument for all primer combinations: 95°C for 30 s, 6 cycles of 95°C for 3 s, 68°C for 20 s (−1°C per cycle), 72°C for 1 s, and 34 cycles of 95°C for 3 s, 62°C for 20 s, 72°C for 1 s, followed by a melt curve starting at 65°C and ending at 95°C. Mean strain quantities (in ng) were calculated using a standard curves derived from 10-fold dilution curves of 100 ng to 0.1pg of gDNA for each barcoded *B. thetaiotomicron* strain and the efficiency-corrected ΔC_q method (Bookout et al., 2006). Quantities were then transformed into percentages of each barcode within a sample and plotted.

EXCISION qPCR

B. thetaiotaomicron transconjugants with BtCTn and BoCTn were precultured in TYG and grown as above in the liquid growth assays in 5mL of MM + Met and MM + B_{12} (4 nM) and biological triplicate until they reached mid-log phase. Cells were recovered by centrifugation for 10 min at 3,000 × *g* and total genomic DNA was isolated as performed for genomic sequencing above. Samples were analyzed in technical triplicate with qPCR as described above using primer pairs for the 'empty' bacterial attachment site (*attB*), the 'closed' CTn confirmation (*attC*) and the integrated left and right attachment sites (*attL, attR*) (Table S7). Fold differences for each amplicon in each strain between the two media conditions were evaluated using the $\Delta\Delta C_q$ method (Bookout et al., 2006) with *BT1087* as the reference gene. The LinRegPCR v2021.1 program (Ruijter et al. 2009) was used to calculate the starting concentration of each amplicon (N_0), which were in turn used to evaluate the frequency of excision (N_0 *attC*/N_0 *attL* and N_0 *attC*/N_0 *attR*) using a two-way ANOVA.

QUANTIFICATION AND STATISTICAL ANALYSIS

Statistical tests, number of events quantified, standard error of the mean or deviations, and statistical significance is reported in figure legends.

Supplementary Material

Refer to Web version on PubMed Central for supplementary material.

ACKNOWLEDGMENTS

We thank Alvaro Hernandez from the W.M. Keck Center for Comparative and Functional Genomics at the University of Illinois at Urbana-Champaign (UIUC) for technical services; Jonathan Mitchell for maintenance and animal care at the University of California, Riverside (UCR) vivarium; Rachel Whitaker at UIUC for use of the PFGE equipment; and Samson Avena at UCR for assistance screening transconjugants. This research was supported by initial complement funding to P.H.D. from UIUC and UCR and K.F. was supported by the Department of Microbiology at UIUC. Gnotobiotic mouse work and A.H. were supported by NIH/NIGMS grant R35GM124724 and NIH/NIAID grant R01AI157106, to A.H.

REFERENCES

Alvarez-Martinez CE, and Christie PJ (2009). Biological diversity of prokaryotic type IV secretion systems. Microbiol. Mol. Biol. Rev 73, 775–808. [PubMed: 19946141]

Bacic M, Parker AC, Stagg J, Whitley HP, Wells WG, Jacob LA, and Smith CJ (2005). Genetic and structural analysis of the *Bacteroides* conjugative transposon CTn341. J. Bacteriol 187, 2858–2869. [PubMed: 15805532]

Bertram J, Strätz M, and Dürre P (1991). Natural transfer of conjugative transposon Tn916 between gram-positive and gram-negative bacteria. J. Bacteriol 173, 443–448. [PubMed: 1846142]

Bookout AL, Cummins CL, Kramer MF, Pesola JM, and Mangelsdorf DJ (2006). High-throughput real-time quantitative reverse transcription PCR. Curr. Protoc. Mol. Biol 15. 10.1002/0471142727.

Buckwold SL, Shoemaker NB, Sears CL, and Franco AA (2007). Identification and characterization of conjugative transposons CTn86 and CTn9343 in *Bacteroides fragilis* strains. Appl. Environ. Microbiol 73, 53–63. [PubMed: 17071793]

Buffie CG, and Pamer EG (2013). Microbiota-mediated colonization resistance against intestinal pathogens. Nat. Rev. Immunol 13, 790–801. [PubMed: 24096337]

Burrus V, Pavlovic G, Decaris B, and Guédon G (2002). Conjugative transposons: The tip of the iceberg. Mol. Microbiol 46, 601–610. [PubMed: 12410819]

Campbell DE, Ly LK, Ridlon JM, Hsiao A, Whitaker RJ, and Degnan PH (2020). Infection with *Bacteroides* Phage BV01 alters the host transcriptome and bile acid metabolism in a common human gut microbe. Cell Rep 32, 108142. [PubMed: 32937127]

Carpena N, Manning KA, Dokland T, Marina A, and Penadés JR (2016). Convergent evolution of pathogenicity islands in helper cos phage interference. Phil. Trans. R. Soc. B 371, 20150505. [PubMed: 27672154]

Casjens S, Winn-Stapley DA, Gilcrease EB, Morona R, Kühlewein C, Chua JEH, Manning PA, Inwood W, and Clark AJ (2004). The chromosome of *Shigella flexneri* Bacteriophage Sf6: Complete nucleotide sequence, genetic mosaicism, and DNA packaging. J. Mol. Biol 339, 379–394. [PubMed: 15136040]

Chimento DP, Mohanty AK, Kadner RJ, and Wiener MC (2003). Substrate-induced transmembrane signaling in the cobalamin transporter BtuB. Nat. Struct. Biol 10, 394–401. [PubMed: 12652322]

Clark AJ, Inwood W, Cloutier T, and Dhillon TS (2001). Nucleotide sequence of coliphage HK620 and the evolution of lambdoid phages. J. Mol. Biol 311, 657–679. [PubMed: 11518522]

Costliow ZA, and Degnan PH (2017). Thiamine acquisition strategies impact metabolism and competition in the gut microbe *Bacteroides thetaiotaomicron*. mSystems 2, e00116–e00117. [PubMed: 28951891]

Coyne MJ, Zitomersky NL, Mcguire M, Zitomersky L, Earl AM, and Comstock E (2014). Evidence of extensive DNA transfer between *Bacteroidales* species within the human gut. mBio 5, e01305–e01314. [PubMed: 24939888]

Coyne MJ, Roelofs KG, and Comstock LE (2016).Type VI secretion systems of human gut *Bacteroidales* segregate into three genetic architectures, two of which are contained on mobile genetic elements. BMC Genomics 17, 58. [PubMed: 26768901]

Darling ACE, Mau B, Blattner FR, and Perna NT (2004). Mauve: Multiple alignment of conserved genomic sequence with rearrangements. Genome Res 14, 1394–1403. [PubMed: 15231754]

Deatherage DE, and Barrick JE (2014). Identification of mutations in laboratory-evolved microbes from next-generation sequencing data using breseq. Methods Mol. Biol 1151, 165–188. [PubMed: 24838886]

Degnan PH, and Moran NA (2008). Evolutionary genetics of a defensive facultative symbiont of insects: Exchange of toxin-encoding bacteriophage. Mol. Ecol 17, 916–929. [PubMed: 18179430]

Degnan PH, Taga ME, and Goodman AL (2014a). Vitamin B_{12} as modulator of gut microbial ecology. Cell Metab 20, 769–778. [PubMed: 25440056]

Degnan PH, Barry NA, Mok KC,Taga ME, and Goodman AL (2014b). Human gut microbes use multiple transporters to distinguish vitamin B_{12} analogs and compete in the gut. Cell Host Microbe 15, 47–57. [PubMed: 24439897]

van Dongen S (2000). A Cluster Algorithm for Graphs. Technical Report INS-R0010 (Amsterdam: National Research Institute for Mathematics and Computer Science in the Netherlands).

Duerkop BA, Clements CV, Rollins D, Rodrigues JLM, and Hooper LV (2012). A composite bacteriophage alters colonization by an intestinal commensal bacterium. Proc. Nat. Acad. Sci. USA 109, 17621–17626. [PubMed: 23045666]

Edgar RC (2004). MUSCLE: Multiple sequence alignment with high accuracy and high throughput. Nucl. Acids Res 32, 1792–1797. [PubMed: 15034147]

El-Gebali S, Mistry J, Bateman A, Eddy SR, Luciani A, Potter SC, Qureshi M, Richardson LJ, Salazar GA, Smart A, et al. (2019). The Pfam protein families database in 2019. Nucl. Acids Res 47, D427–D432. [PubMed: 30357350]

Enright AJ (2002). An efficient algorithm for large-scale detection of protein families. Nucl. Acids Res 30, 1575–1584. [PubMed: 11917018]

Di Girolamo PM, and Bradbeer C (1971). Transport of vitamin B_{12} in *Escherichia coli*. J. Bacteriol 106, 745–750. [PubMed: 4934062]

Goodman AL, McNulty NP, Zhao Y, Leip D, Mitra RD, Lozupone CA, Knight R, and Gordon JI (2009). Identifying genetic determinants needed to establish a human gut symbiont in its habitat. Cell Host Microbe 6, 279–289. [PubMed: 19748469]

Gupta A, Vlamakis H, Shoemaker N, and Salyers AA (2003). A new *Bacteroides* conjugative transposon that carries an *ermB* gene. Appl. Environ. Microbiol 69, 6455–6463. [PubMed: 14602600]

Haft DH (2001).TIGRFAMs:A protein family resource for the functional identification of proteins. Nucl. Acids Res 29, 41–43. [PubMed: 11125044]

Hehemann JH, Correc G, Barbeyron T, Helbert W, Czjzek M, and Michel G (2010).Transfer of carbohydrate-active enzymes from marine bacteria to Japanese gut microbiota. Nature 464, 908–912. [PubMed: 20376150]

Hehemann J-H, Kelly AG, Pudlo NA, Martens EC, and Boraston AB (2012). Bacteria of the human gut microbiome catabolize red seaweed glycans with carbohydrate-active enzyme updates from extrinsic microbes. Proc. Nat. Acad. Sci. USA 109, 19786–19791. [PubMed: 23150581]

Holdeman LV, Cato EP, and Moore WEC (1977). Anaerobic Laboratory Manual, 4th Edition (Blacksburg: Anaerobe Laboratory, Virginia Polytechnic Institute and State University).

Hong SN, and Rhee PL (2014). Unraveling the ties between irritable bowel syndrome and intestinal microbiota. World J. Gastroentero 20, 2470–2481.

Husain F, Veeranagouda Y, Boente R, Tang K, Mulato G, and Wexler HM (2014). The Ellis Island effect: A novel mobile element in a multi-drug resistant *Bacteroides fragilis* clinical isolate includes a mosaic of resistance genes from Gram-positive bacteria. Mob. Genet. Elem 4, e29801.

Jacobson A, Lam L, Rajendram M, Tamburini F, Honeycutt J, Pham T, Van Treuren W, Pruss K, Stabler SR, Lugo K, et al. (2018). A gut commensal-produced metabolite mediates colonization resistance to *Salmonella* infection. Cell Host Microbe 24, 296–307. [PubMed: 30057174]

John GK, and Mullin GE (2016). The gut microbiome and obesity. Curr. Oncol. Rep 18, 45. [PubMed: 27255389]

Johnson CM, and Grossman AD (2016). The composition of the cell envelope affects conjugation in *Bacillus subtilis*. J. Bacteriol 198, 1241–1249. [PubMed: 26833415]

Juhala RJ, Ford ME, Duda RL, Youlton A, Hatfull GF, and Hendrix RW (2000). Genomic sequences of bacteriophages HK97 and HK022: pervasive genetic mosaicism in the lambdoid bacteriophages. J. Mol. Biol 299, 27–51. [PubMed: 10860721]

Kamada N, Kim Y-G, Sham HP, Vallance BA, Puente JL, Martens EC, and Nunez G (2012). Regulated virulence controls the ability of a pathogen to compete with the gut microbiota. Science 336, 1325–1329. [PubMed: 22582016]

Kenley JS, Leighton M, and Bradbeer C (1978). Transport of vitamin B_{12} in *Escherichia coli*: Corrinoid specificity of the outer membrane receptor. J. Biol. Chem 253, 1341–1346. [PubMed: 342525]

Koropatkin NM, Martens EC, Gordon JI, and Smith TJ (2008). Starch catabolism by a prominent human gut symbiont is directed by the recognition of amylose helices. Structure 16, 1105–1115. [PubMed: 18611383]

Litvak Y, and Bäumler AJ (2019). The founder hypothesis: A basis for microbiota resistance, diversity in taxa carriage, and colonization resistance against pathogens. PLoS Pathog 15, e1007563. [PubMed: 30789972]

Martens EC, Chiang HC, and Gordon JI (2008). Mucosal glycan foraging enhances fitness and transmission of a saccharolytic human gut bacterial symbiont. Cell Host Microbe 4, 447–457. [PubMed: 18996345]

Meehan CJ, and Beiko RG (2012). Lateral gene transfer of an ABC transporter complex between major constituents of the human gut microbiome. BMC Microbiol 12, 248. [PubMed: 23116195]

Miller MA, Pfeiffer W, and Schwartz T (2010). Creating the CIPRES Science Gateway for inference of large phylogenetic trees. In 2010 Gateway Computing Environments Workshop (GCE), (New Orleans, LA, USA: IEEE), pp. 1–8.

O'Brien A, Newland J, Miller S, Holmes R, Smith H, and Formal S (1984). Shiga-like toxin-converting phages from *Escherichia coli* strains that cause hemorrhagic colitis or infantile diarrhea. Science 226, 694–696. [PubMed: 6387911]

Quesada-Gómez C (2011). *Bacteroides* mobilizable and conjugative genetic elements: Antibiotic resistance among clinical isolates. Rev. Esp. Quimioter 24, 184–190. [PubMed: 22173187]

Rankin DJ, Rocha EPC, and Brown SP (2011). What traits are carried on mobile genetic elements, and why? Heredity 106, 1–10. [PubMed: 20332804]

Rice P, Longden L, and Bleasby A (2000). EMBOSS: The European molecular biology open software suite. Trends Genet 16, 276–277. [PubMed: 10827456]

Riley AB, Kim D, and Hansen AK (2017). Genome sequence of "*Candidatus* Carsonella ruddii" strain BC, a nutritional endosymbiont of *Bactericera cockerelli*. Genome Announc 5, e00217–e00236. [PubMed: 28450506]

Roth JR, Lawrence JG, and Bobik TA (1996). Cobalamin (coenzyme B_{12}): Synthesis and biological significance. Ann. Rev. Microbiol 50, 137–181. [PubMed: 8905078]

Rowland I, Gibson G, Heinken A, Scott K, Swann J, Thiele I, and Tuohy K (2018). Gut microbiota functions: Metabolism of nutrients and other food components. Eur. J. Nutr 57, 1–24.

Ruijter JM, Ramakers C, Hoogaars WMH, Karlen Y, Bakker O, van den Hoff MJB, and Moorman AFM (2009). Amplification efficiency: Linking baseline and bias in the analysis of quantitative PCR data. Nucleic Acids Res 37, e45. [PubMed: 19237396]

Salyers AA, and Shoemaker NB (1994). Broad-host-range gene transfer plasmids and conjugative transposons. FEMS Microbiol. Ecol 15, 15–22.

Salyers A, Gupta A, and Wang Y (2004). Human intestinal bacteria as reservoirs for antibiotic resistance genes. Trends Microbiol 12, 412–416. [PubMed: 15337162]

Scott KP (2002). The role of conjugative transposons in spreading antibiotic resistance between bacteria that inhabit the gastrointestinal tract. Cell. Mol. Life Sci 59, 2071–2082. [PubMed: 12568333]

Sequeira RP, McDonald JAK, Marchesi JR, and Clarke TB (2020). Commensal Bacteroidetes protect against *Klebsiella pneumoniae* colonization and transmission through IL-36 signalling. Nat. Microbiol 5, 304–313. [PubMed: 31907407]

Shannon P (2003). Cytoscape: A software environment for integrated models of biomolecular interaction networks. Genome Res 13, 2498–2504. [PubMed: 14597658]

Shkoporov AN, Khokhlova EV, Kulagina EV, Smeianov VV, Kuchmiy AA, Kafarskaya LI, and Efimov BA (2013). Analysis of a novel 8.9kb cryptic plasmid from *Bacteroides uniformis*, its long-term stability and spread within human microbiota. Plasmid 69, 146–159. [PubMed: 23201047]

Shoemaker NB, Vlamakis H, Hayes K, and Salyers AA (2001). Evidence for extensive resistance gene transfer among *Bacteroides* spp. and among *Bacteroides* and other genera in the human colon. Appl. Environ. Microbiol 67, 561–568. [PubMed: 11157217]

Sommer F, and Bäckhed F (2013). The gut microbiota – masters of host development and physiology. Nat. Rev. Microbiol 11, 227–238. [PubMed: 23435359]

Stamatakis A (2006). RAxML-VI-HPC: maximum likelihood-based phylogenetic analyses with thousands of taxa and mixed models. Bioinformatics 22, 2688–2690. [PubMed: 16928733]

Stecher B, Denzler R, Maier L, Bernet F, Sanders MJ, Pickard DJ, Barthel M, Westendorf AM, Krogfelt KA, Walker AW, et al. (2012). Gut inflammation can boost horizontal gene transfer between pathogenic and commensal Enterobacteriaceae. Proc. Nat. Acad. Sci. USA 109, 1269–1274. [PubMed: 22232693]

The Human Microbiome Project (2012). Structure, function and diversity of the healthy human microbiome. Nature 486, 207–214. [PubMed: 22699609]

Top EM, and Springael D (2003). The role of mobile genetic elements in bacterial adaptation to xenobiotic organic compounds. Curr. Opin. Biotech 14, 262–269. [PubMed: 12849778]

Tribble GD, Parker AC, and Smith CJ (1999). Genetic structure and transcriptional analysis of a mobilizable, antibiotic resistance transposon from Bacteroides. Plasmid 42, 1–12. [PubMed: 10413660]

Trieu-Cuot P, Carlier C, and Courvalin P (1988). Conjugative plasmid transfer from *Enterococcus faecalis* to *Escherichia coli*. J. Bacteriol 170, 4388–4391. [PubMed: 3137216]

Truett GE, Heeger P, Mynatt RL, Truett AA, Walker JA, and Warman ML (2000). Preparation of PCR-quality mouse genomic DNA with hot sodium hydroxide and tris (HotSHOT). BioTechniques 29, 52–54. [PubMed: 10907076]

Varel VH, and Bryant MP (1974). Nutritional features of *Bacteroides fragilis* subsp. *fragilis*. Appl. Microbiol 28, 251–257. [PubMed: 4853401]

Visconti A, Le Roy CI, Rosa F, Rossi N, Martin TC, Mohney RP, Li W, de Rinaldis E, Bell JT, Venter JC, et al. (2019). Interplay between the human gut microbiome and host metabolism. Nat. Commun 10, 4505. [PubMed: 31582752]

Waldor MK, and Mekalanos JJ (1996). Lysogenic conversion by a filamentous phage encoding cholera toxin. Science 272, 1910–1914. [PubMed: 8658163]

Wang J, Shoemaker NB, Wang GR, and Salyers AA (2000). Characterization of a *Bacteroides* mobilizable transposon, NBU2, which carries a functional lincomycin resistance gene. J. Bacteriol 182, 3559–3571. [PubMed: 10852890]

Wang Y, Shoemaker NB, and Salyers AA (2004). Regulation of a *Bacteroides* operon that controls excision and rransfer of the conjugative transposon CTnDOT. J. Bacteriol 186, 2548–2557. [PubMed: 15090494]

Wang GR, Shoemaker NB, Jeters RT, and Salyers AA (2011). CTn12256, a chimeric *Bacteroides* conjugative transposon that consists of two independently active mobile elements. Plasmid 66, 93–105. [PubMed: 21777612]

Welch RA, Jones KR, and Macrina FL (1979). Transferable lincosamide-macrolide resistance in *Bacteroides*. Plasmid 2, 261–268. [PubMed: 451051]

Wesslund NA, Wang GR, Song B, Shoemaker NB, and Salyers AA (2007). Integration and excision of a newly discovered *Bacteroides* conjugative transposon, CTnBST. J. Bacteriol 189, 1072–1082. [PubMed: 17122349]

Wexler AG, Schofield WB, Degnan PH, Folta-Stogniew E, Barry NA, and Goodman AL (2018). Human gut *Bacteroides* capture vitamin B_{12} via cell surface-exposed lipoproteins. eLife 7, 1–20.

Whittle G, Shoemaker NB, and Salyers AA (2002). The role of *Bacteroides* conjugative transposons in the dissemination of antibiotic resistance genes. Cell. Mol. Life Sci 59, 2044–2054. [PubMed: 12568330]

Wikoff WR, Anfora AT, Liu J, Schultz PG, Lesley SA, Peters EC, and Siuzdak G (2009). Metabolomics analysis reveals large effects of gut microflora on mammalian blood metabolites. Proc. Nat. Acad. Sci. USA 106, 3698–3703. [PubMed: 19234110]

Wu M, McNulty NP, Rodionov DA, Khoroshkin MS, Griffin NW, Cheng J, Latreille P, Kerstetter RA, Terrapon N, Henrissat B, et al. (2015). Genetic determinants of *in vivo* fitness and diet responsiveness in multiple human gut *Bacteroides*. Science 350, aac5992. [PubMed: 26430127]

Yi S, Seth EC, Men YJ, Stabler SP, Allen RH, Alvarez-Cohen L, and Taga ME (2012). Versatility in corrinoid salvaging and remodeling pathways supports corrinoid-dependent metabolism in *Dehalococcoides mccartyi*. Appl. Environ. Microbiol 78, 7745–7752. [PubMed: 22923412]

Zhang Y, Rodionov DA, Gelfand MS, and Gladyshev VN (2009). Comparative genomic analyses of nickel, cobalt and vitamin B_{12} utilization. BMC Genomics 10, 78. [PubMed: 19208259]

Zhao S, Lieberman TD, Poyet M, Kauffman KM, Gibbons SM, Groussin M, Xavier RJ, and Alm EJ (2019). Adaptive evolution within gut microbiomes of healthy people. Cell Host Microbe 25, 656–667.e8. [PubMed: 31028005]

Allen RH, and Stabler SP (2008). Identification and quantitation of cobalamin and cobalamin analogues in human feces. Am. J. Clin. Nutr 87, 1324–1335. [PubMed: 18469256]

Highlights

- Diverse mobile genetic elements in gut microbes encode vitamin B_{12} transporters
- Transfer of CTns with B_{12} transporters complement transport-deficient strains
- CTns with B_{12} transporters offer competitive advantages during *in vitro* growth
- *In vivo* conjugation restores ability to use B_{12} in transport-deficient *Bacteroides*

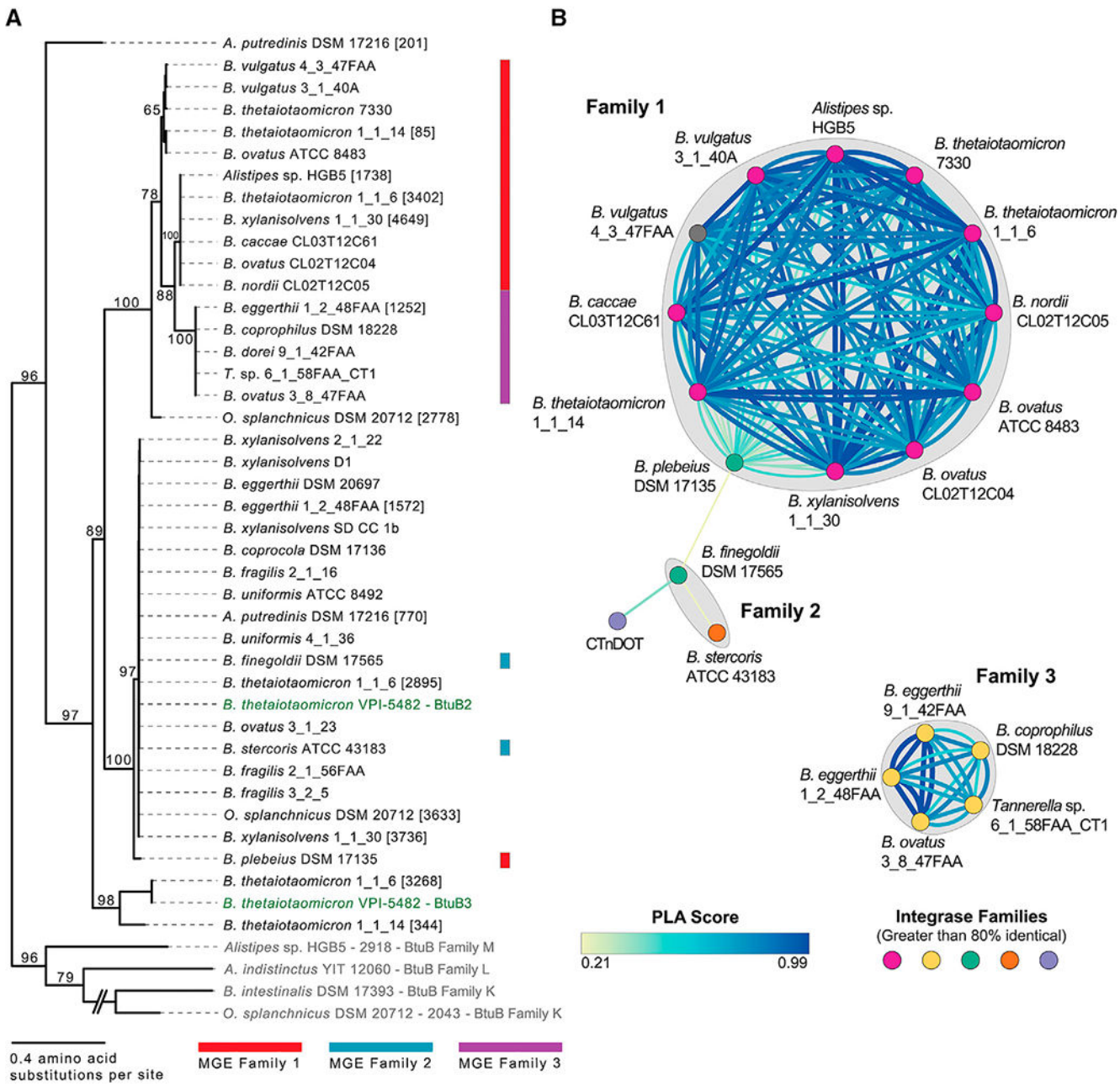

Figure 1. Predicted corrinoid transport-encoding MGEs encode similar BtuB alleles and group into three distinct families

(A) Maximum likelihood phylogeny of chromosomal and mobilizable gut Bacteroidetes BtuB alleles. All MGE-encoded BtuB alleles cluster within BtuB Family N. Representatives of Families K, L, and M are included as outgroups (gray). Chromosomally encoded BtuB2 and BtuB3 from *B. thetaiotaomicron* VPI-5482 are in green and the MGE family groupings are noted by colored blocks. Species with multiple BtuB alleles represented contain gene identifiers in brackets. Bootstrap values are shown.

(B) Predicted MGE families were inferred by the MCL algorithm based on the PLA between each MGE. Edge widths and colors connecting each of the nodes represent the similarity

between MGEs. CTnDOT was included for reference. Nodes are colored by the amino acid identity of the MGE integrase with a gray node indicating no integrase was detected. See also Figures S1–S4.

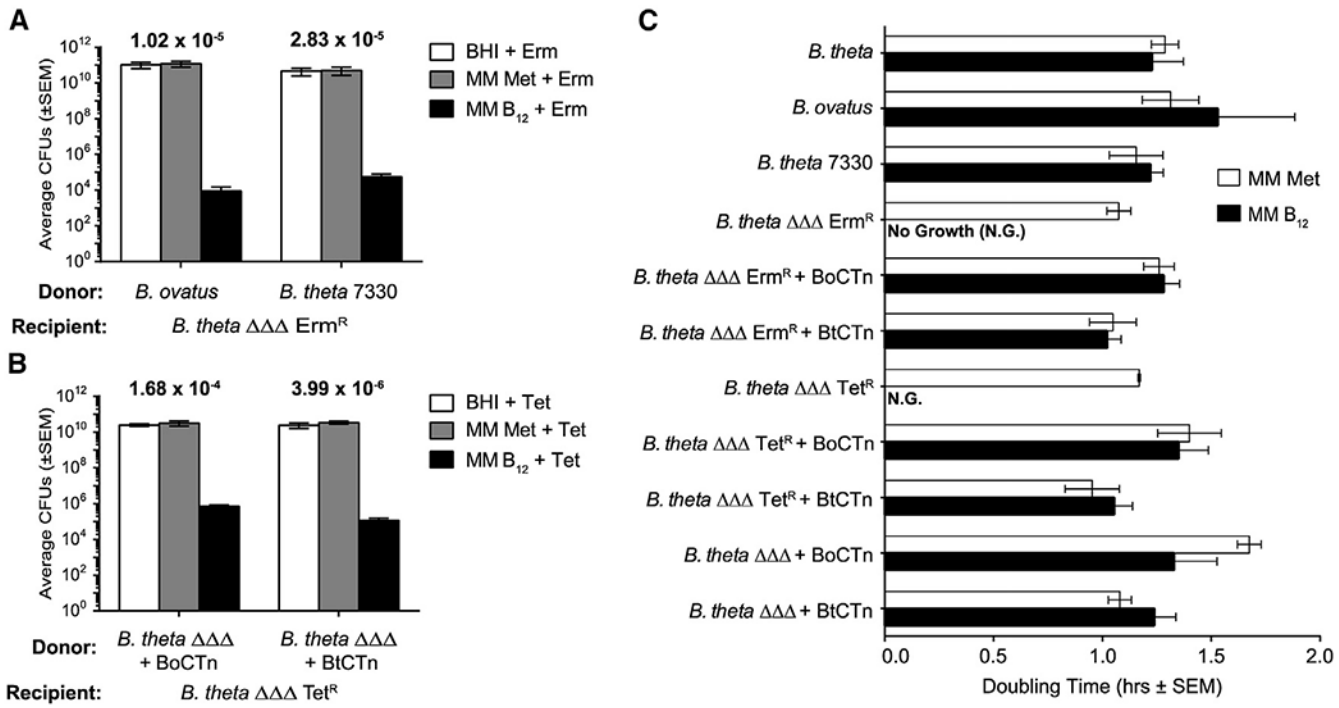

Figure 2. Predicted MGEs BoCTn and BtCTn are mobilizable and transport vitamin B_{12}

(A) Initial conjugations were performed between native MGE-host strains *B. ovatus* ATCC 8483 and *B. thetaiotaomicron* 7330 and recipient strain *B. thetaiotaomicron* ΔΔΔ Erm^R. Successful *B. thetaiotaomicron* ΔΔΔ transconjugants for both BoCTn and BtCTn were isolated on minimal media containing vitamin B_{12} and erythromycin.

(B) Secondary conjugations between BoCTn or BtCTn encoding transconjugants and *B. thetaiotaomicron* ΔΔΔ Tet^R recipients were performed to investigate if the first transfer of the CTn included all the necessary elements for repeated transfer of the element. Successful *B. thetaiotaomicron* ΔΔΔ transconjugants for both BoCTn and BtCTn were isolated on minimal media containing vitamin B_{12} and tetracycline. Transfer frequencies for each conjugation are denoted above each section of bars.

(C) Parent, recipient, and representative initial and secondary transconjugant strains were grown in MM + Met and MM + B_{12}. Recipient triple-locus deletion strains (*B. theta* ΔΔΔ Erm^R and Tet^R) are incapable of growing in the presence of vitamin B_{12}, while all parental strains and transconjugants are capable. Values represent the average and standard error of the mean for four biological replicates (A and B) or biological triplicates (C).

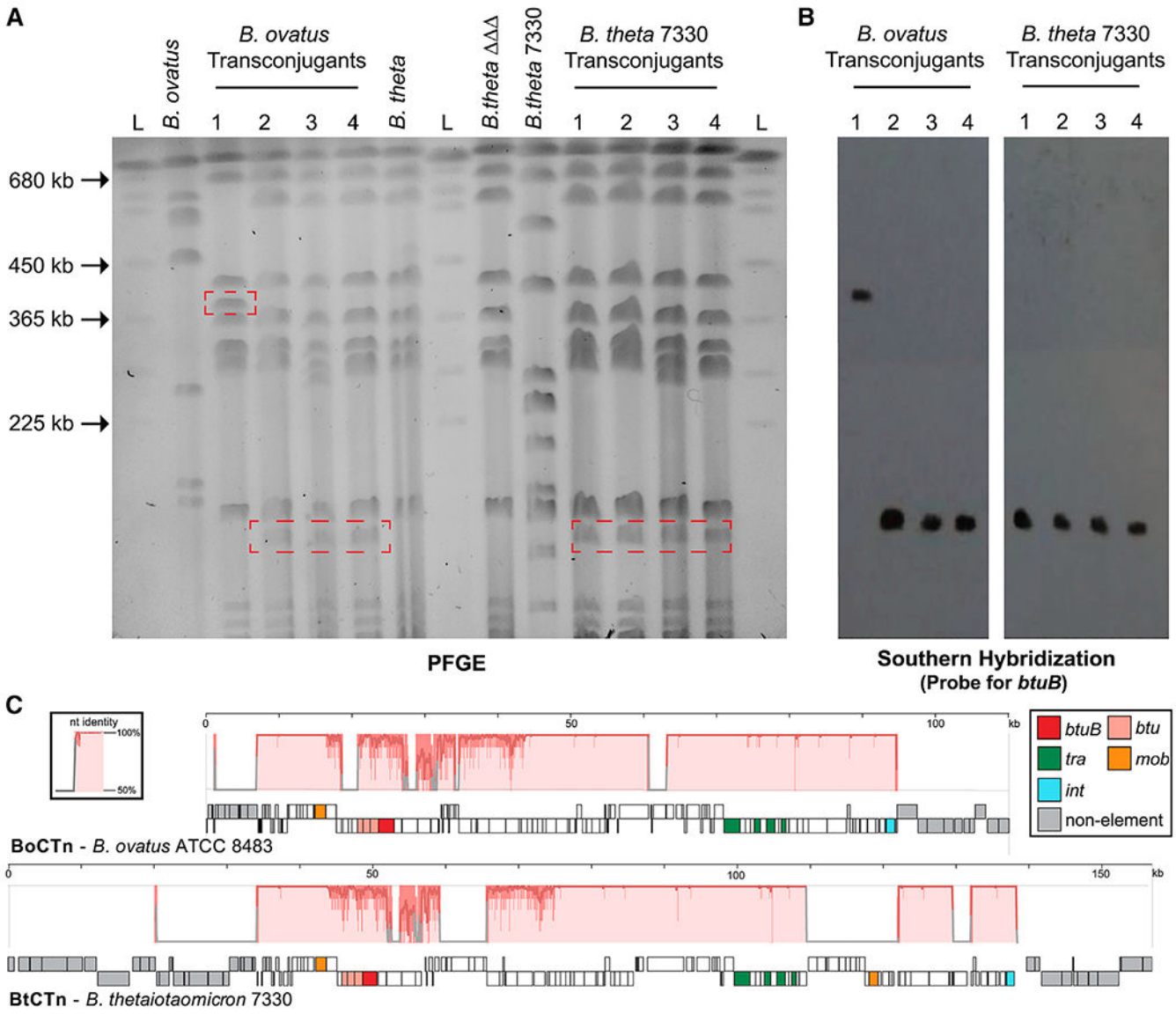

Figure 3. BoCTn and BtCTn transfers are detected by PFGE and Southern hybridization

(A) PFGE of wild-type *B. thetaiotaomicron*, donor (*B. ovatus* and *B. thetaiotaomicron* 7330), recipient (*B. thetaiotaomicron* ΔΔΔ), and representative transconjugants. Transconjugant genome fingerprints match the recipient with the exception of evidence of CTn insertion (red dotted boxes). L signifies the Ladder lanes.

(B) Corresponding Southern hybridizations of PFGE gel in A with probes specific to *btuB*.

(C) Nucleotide alignments of BoCTn and BtCTn (including their flanking regions) have a single locally conserved block as aligned by Mauve. Shared regions have ≥80% nucleotide sequence identity as indicated by the similarity profile. Genes of note are colored according to the key and further details are available in Table S6. See Figure S5 for the consensus attachment site sequences.

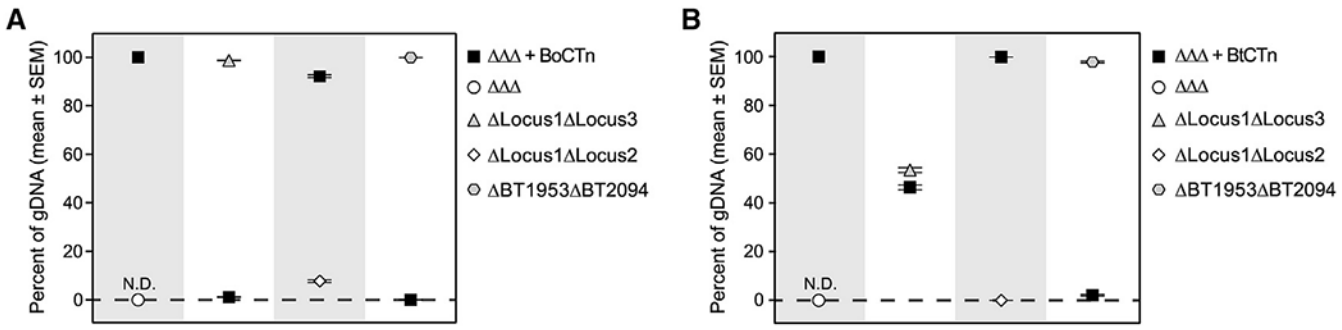

Figure 4. Transconjugants have intermediate competitive advantages compared with *B. thetaiotaomicron* VPI-5482 chromosomal *btu* loci

Competitions were performed between *B. thetaiotaomicron* ΔΔΔ + BoCTn (A) or BtCTn (B) and *B. thetaiotaomicron* ΔΔΔ, ΔLocus1ΔLocus3 (Locus 2), ΔLocus1ΔLocus2 (Locus 3), or ΔBT1953ΔBT2094 (*btuB*1, *btuFCD*2/3). Competitions were performed over 5 days in MM + B_{12} with serial passaging every 24 h. Strain abundances were determined by qPCR and are represented by percent of genomic DNA (gDNA). Error bars represent the standard error of the mean from three technical qPCR replicates of three technical competition replicates. See also Figure S6.

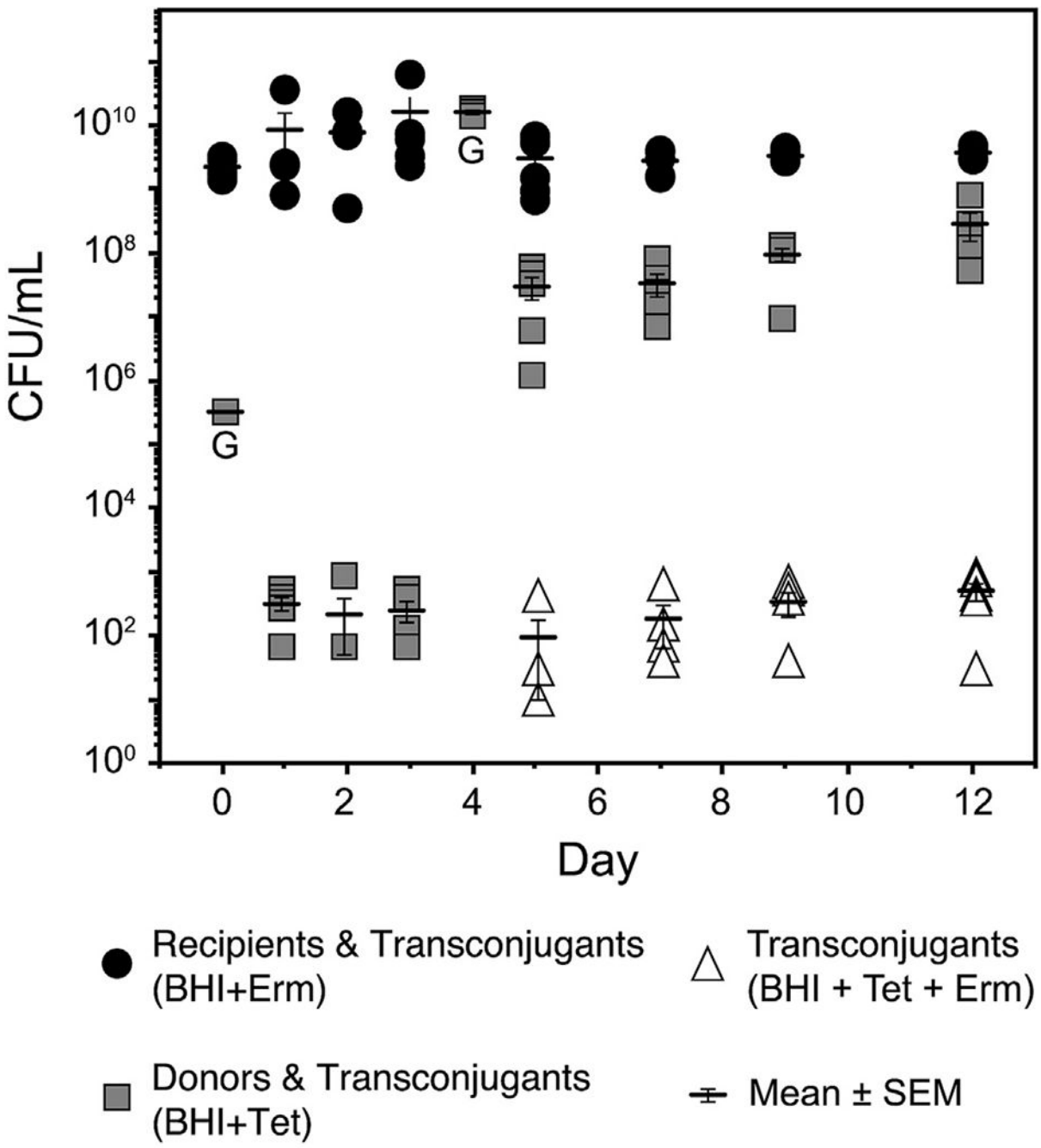

Figure 5. BoCTn and BtCTn can mobilize within the mammalian intestine

Germ-free mice were initially colonized with recipient *B. thetaiotaomicron* ΔΔΔ Erm^R 2 days prior to introduction of donor cells (day −2). On day 0, equal portions (G, gavage sample) of donor strains *B. thetaiotaomicron* ΔΔΔ + BoCTn_Tet^R and *B. thetaiotaomicron* ΔΔΔ + BtCTn_Tet^R were introduced to the mice colonized by *B. thetaiotaomicron* ΔΔΔ Erm^R recipient cells. At days 0, 1, 3, 5, 7, 9, and 12, fecal samples were collected and plated on Brain Heart Infusion (BHI) + Tet + Gn, BHI + Erm + Gn, and BHI + Erm + Tet + Gn for CFUs. On day 4, a second gavage (G) of the donor strains was administered. Starting on day

5, transconjugants were observed (triangles). Mean calculated transfer frequencies for each day were: day 5 ~9.7×10^{-9}, day 7 ~3.3×10^{-8}, day 9 ~1.0×10^{-7} and day 12 ~8.2×10^{-8}. Mean CFU/mL based on two or three replicates; standard error of the mean based on five mice. See also Figure S7.

Cell Rep. Author manuscript; available in PMC 2022 January 14.

Table 1.

Predicted corrinoid transport-encoding MGEs

Organism	BtuB	BtuB phylogeny group	Total length (bp)
MGE Family 1 (ACTAAATTTACCAGATTT/ACTAAATTTACCAGATTT)[a]			
Bacteroides ovatus ATCC 8483	BACOVA04705	1	87,773
Bacteroides thetaiotaomicron 7330	Bthe7332330	1	104,197
Bacteroides thetaiotaomicron 1_1_14	HMPREF900700085	1	86,150
Bacteroides vulgatus 3_1_40A	HMPREF901104185	1	86,906
Bacteroides vulgatus 4_3_47FAA[c]	BSFG02809	1	77,507
Alistipes sp. HGB5	HMPREF97201738	2	76,410
Bacteroides caccae CL03T12C61	HMPREF106100371	2	106,936
Bacteroides nordii CL02T12C05[c]	HMPREF106800063	2	107,262
Bacteroides ovatus CL02T12C04	HMPREF106902364	2	94,150
Bacteroides thetaiotaomicron 1_1_6	BSIG03402	2	76,411
Bacteroides xylanisolvens 1_1_30	HMPREF012704649	2	76,412
Bacteroides plebeius DSM 17135[b]	BACPLE02589	3	93,364
MGE Family 2 (GCGG/GCGG)[a]			
Bacteroides finegoldii DSM 17565	BACFIN05187	3	137,152
Bacteroides stercoris ATCC 43183	BACSTE00795	3	82,529
MGE Family 3 (GGCARAC/CTRTGCC)[a]			
Bacteroides coprophilus DSM 18228	BACCOPRO02034	4	106,761
Bacteroides dorei 9_1_42FAA	BSBG01238	4	158,110
Bacteroides eggerthii 1_2_48FAA[c]	HMPREF101601252	4	158,130
Bacteroides ovatus 3_8_47FAA[c]	HMPREF101701627	4	158,569
Tannerella sp. 6_1_58FAA_CT1	HMPREF103300160	4	169,829

[a]Consenus predicted *attL/attR* sites.

[b]Possesses nonconsensus *attL/attR*.

$c_{\text{MGE split on two different contigs.}}$

Table 2.

Bacterial strains used in this study

	Relevant phenotype		
Shortname in text	**CTn**	**B_{12} transport**	**Resistance**
Parental and recipient strains:			
Bacteroides thetaiotaomicron	−	+	−
B. thetaiotaomicron Erm^R	−	+	Erm^R
Bacteroides ovatus	BoCTn	+	−
B. thetaiotaomicron 7330	BtCTn	+	−
B. thetaiotaomicron ΔΔΔ	−	−	−
B. thetaiotaomicron ΔΔΔ Erm^R	−	−	Erm^R
B. thetaiotaomicron ΔΔΔ Tet^R	−	−	Tet^R
Transconjugants from parental strains:			
B. thetaiotaomicron ΔΔΔ Erm^R + BoCTn	BoCTn	+	Erm^R
B. thetaiotaomicron ΔΔΔ Erm^R + BtCTn	BtCTn	+	Erm^R
Transconjugants from transconjugant strains:			
B. thetaiotaomicron ΔΔΔ Tet^R + BoCTn	BoCTn	+	Tet^R
B. thetaiotaomicron ΔΔΔ Tet^R + BtCTn	BtCTn	+	Tet^R
Unmarked transconjugant strains:			
B. thetaiotaomicron ΔΔΔ + BoCTn	BoCTn	+	−
B. thetaiotaomicron ΔΔΔ + BtCTn	BtCTn	+	−
Barcoded strains for competitions:			
B. thetaiotaomicron Δ*locus1* Δ*locus3* BC	−	+, *locus2* only	Tet^R
B. thetaiotaomicron Δ*locus1* Δ*locus2* BC	−	+, *locus3* only	Tet^R
B. thetaiotaomicron Δ*BT1953*Δ*BT2094* BC	−	+, *locus1 btuB*	Tet^R
B. thetaiotaomicron ΔΔΔ BC			
B. thetaiotaomicron ΔΔΔ + BoCTn BC	BoCTn	+	Tet^R
B. thetaiotaomicron ΔΔΔ + BtCTn BC	BtCTn	+	Tet^R
Strains carrying tetracyline resistance marked CTns:			

Shortname in text	Relevant phenotype		
	CTn	B_{12} transport	Resistance
B. thetaiotaomicron ΔΔΔ + BoCTn_Tet^R	BoCTn	+	Tet^R
B. thetaiotaomicron ΔΔΔ + BtCTn_Tet^R	BtCTn	+	Tet^R
Transconjugants isolated from the mouse gut:			
Mouse-isolated BoCTn TC-1	BoCTn	+	Erm^R, Tet^R
Mouse-isolated BoCTn TC-2	BoCTn	+	Erm^R, Tet^R
Mouse-isolated BtCTn TC-1	BtCTn	+	Erm^R, Tet^R
Mouse-isolated BtCTn TC-2	BtCTn	+	Erm^R, Tet^R

KEY RESOURCES TABLE

REAGENT or RESOURCE	SOURCE	IDENTIFIER
Bacterial and virus strains		
B. ovatus ATCC 8483	ATCC	ATCC 8483
B. thetaiotaomicron 7330	Wu et al., 2015	N/A
B. thetaiotaomicron VPI-5482 Δ*tdk* Δ*locus1*Δ*locus2*Δ*locus3*	Degnan et al., 2014b	N/A
B. thetaiotaomicron VPI-5482 Δ*tdk* Δ*locus1*Δ*locus2*Δ*locus3 att1::pNBU2-bla-ermGb*	This study	N/A
B. thetaiotaomicron VPI-5482 Δ*tdk* Δ*locus1*Δ*locus2*Δ*locus3 att2::pNBU2-bla-tetQ*	This study	N/A
B. thetaiotaomicron VPI-5482 Δ*tdk* Δ*locus1*Δ*locus2*Δ*locus3 att1*::pNBU2-bla-ermGb + BoCTn	This study	N/A
B. thetaiotaomicron VPI-5482 Δ*tdk* Δ*locus1*Δ*locus2*Δ*locus3 att1*::pNBU2-bla-ermGb + BtCTn	This study	N/A
B. thetaiotaomicron VPI-5482 Δ*tdk* Δ*locus1*Δ*locus2*Δ*locus3 att2*::pNBU2-bla-tetQ + BoCTn	This study	N/A
B. thetaiotaomicron VPI-5482 Δ*tdk* Δ*locus1*Δ*locus2*Δ*locus3 att2*::pNBU2-bla-tetQ + BtCTn	This study	N/A
B. thetaiotaomicron VPI-5482 Δ*tdk* Δ*locus1*Δ*locus2*Δ*locus3* + BoCTn	This study	N/A
B. thetaiotaomicron VPI-5482 Δ*tdk* Δ*locus1*Δ*locus2*Δ*locus3* + BtCTn	This study	N/A
B. thetaiotaomicron VPI-5482 Δ*tdk* Δ*locus1*Δ*locus2*Δ*locus3* + BoCTn_tetQ	This study	N/A
B. thetaiotaomicron VPI-5482 Δ*tdk* Δ*locus1*Δ*locus2*Δ*locus3* + BtCTn_tetQ	This study	N/A
Biological samples		
Yeast Chromosomal PFG-Marker Mid-Range ladder	New England BioLabs	Cat. #N0345
Critical commercial assays		
Nextera XT Library Preparation Kit	Illumina	Cat. #FC-131-1096
Nextera XT Index Kit	Illumina	Cat. #FC-131-1002
Chemiluminescent Nucleic Acid Detection Module Kit	Thermo Fisher Scientific	Cat. #89880
KAPA SYBR Fast Master Mix	Roche	Cat. #KK4601
Deposited data		
Bacterial genomes, see Table S2	This study	PRJNA715234
Transconjugant genome DNA sequencing, see Table S5	This study	PRJNA715234
Experimental models: Organisms/strains		
Germfree C57BL/6J mice	UCR Gnotobiotic Facility	N/A
Oligonucleotides		
Primers for screening transconjugants, see Table S7	This study	N/A
Primers for strain construction, see Table S7	This study	N/A
Probe for detection of *btuB*, see Table S7	This study	N/A
Primers for excision detection, see Table S7	This study	N/A
Recombinant DNA		
pXchange_BT4111/BT4112, see Data S1	This study	N/A
pXchange_tdk_BoCTn_TetQ, see Data S1	This study	N/A

REAGENT or RESOURCE	SOURCE	IDENTIFIER
pXchange_tdk_BtCTn_TetQ, see Data S1	This study	N/A
pNBU2-bla-ermGb	Koropatkin et al., 2008	N/A
pNBU2-bla-tetQ	Martens et al., 2008	N/A
pNBU2_tet_BC01,04,06,08	Degnan et al., 2014b	N/A
pNBU2_tet_BC09	Costliow and Degnan 2017	N/A
pNBU2_tet_BC14	Martens et al., 2008	N/A
Software and algorithms		
Breseq v0.33.2	Deatherage and Barrick, 2014	https://github.com/barricklab/breseq
A5ud v1	Riley et al., 2017	http://github.com/phdegnan/A5ud https://doi.org/10.5281/zenodo.5712008